

# Ostracods, rock facies and magnetic susceptibility of the Hanonet Formation / Trois-Fontaines Formation boundary interval (Early Givetian) at the Mont d'Haur (Givet, France)

by Jean-Georges CASIER, Xavier DEVLEESCHOUWER, Estelle PETITCLERC & Alain PRÉAT

CASIER, J.-G., DEVLEESCHOUWER, X., PETITCLERC, E. & PRÉAT, A., 2011 – Ostracods, rock facies and magnetic susceptibility of the Hanonet Formation / Trois-Fontaines Formation boundary interval (Early Givetian) at the Mont d'Haur (Givet, France). *Bulletin de l'Institut royal des Sciences naturelles de Belgique, Sciences de la Terre*, 81: 63-96, 5 pls., 4 figs, 1 table, Brussels, November 30, 2011 – ISSN 0374-6291.

## Abstract

Approximately 870 carapaces, valves and fragments of ostracods were extracted from 26 samples collected in the Hanonet Formation (= Fm) and Trois-Fontaines Fm in a section located along the southwestern rampart of the historically entrenched military camp at the Mont d'Haur (Givet, France). Forty-eight species belonging to the Eifelian Mega-Assemblage have been identified and three new are proposed: *Coryellina? audiarti* nov. sp., *Cavellina haursensis* nov. sp. and *Parabolbinella coeni* nov. sp. The ostracod assemblages are generally indicative of shallow marine well-oxygenated environments, except at the base of the Trois-Fontaines Fm where ostracods indicative of semi-restricted and even of lagoonal water conditions are reported.

The sedimentary record represents a transition from mixed siliciclastic-carbonate open-marine ramp system to restricted carbonate platform with deposition in low-energy peritidal and lagoonal settings frequently affected by subaerial exposition. A general trend follows a shallowing-upward and a relative sea-level decrease from the Hanonet Fm toward the Trois-Fontaines Fm. High-energy characterized the ramp setting and destroyed most of the stromatoporoid and coral buildups, which occur as floatstone and rudstone accumulations forming a thick biostrome. *Girvanella* and issinellid shoals developed also in this high-energy environment.

The low-field magnetic susceptibility (=MS) log plotted against the lithological column reveals four magnetic sequences. The MS log and microfacies are moderately correlated mainly due to the evolution of sedimentary environments from a ramp to a platform. The MS values of the Trois-Fontaines Fm are very low in the biostromal unit whereas restricted lagoonal facies are characterized by the highest values of MS. A high-resolution stratigraphic correlative pattern is proposed here between the Mont d'Haur section and the 40 km-distant Baileux section despite the greater thickness. The MS signal is strongly controlled by minerals of ferromagnetic characteristics with a minor contribution of paramagnetic phases. The lagoonal sediments of the Trois-Fontaines Fm are characterized also by

the highest values of normalized viscosity coefficient and a IRM loss. These results confirm the occurrence of a significantly high proportion of ultrafine magnetic grains which may be formed during diagenesis by chemical remanent magnetization processes.

The list of the Givetian ostracods figured by COEN (1985) and recently lodged at the Department of Paleontology at the Royal Belgian Institute of Natural Sciences is reported in annex with new inventory numbers.

**Keywords:** Ostracods, Sedimentology, Paleoecology, Magnetic susceptibility, Early Givetian, Dinant Synclinorium, Ardennes, France.

## Résumé

Environ 870 carapaces, valves et fragments d'ostracodes ont été extraits de 26 échantillons récoltés dans le sommet de la Formation d'Hanonet et dans l'extrême base de la Formation des Trois-Fontaines, au Mont d'Haur (Givet, France). La coupe étudiée est située à proximité des remparts sud-ouest du camp militaire retranché construit par Vauban au XVII<sup>e</sup> siècle. Quarante-sept espèces d'ostracodes appartenant au Méga-Assemblage de l'Eifel sont reconnues et trois nouvelles sont proposées: *Coryellina? audiarti* nov. sp., *Cavellina haursensis* nov. sp. et *Parabolbinella coeni* nov. sp. La faune d'ostracodes recueillie appartient au Méga-Assemblage de l'Eifel et elle indique généralement des milieux marins peu profonds et bien oxygénés. Exceptionnellement dans la base de la Formation de Trois-Fontaines, la présence d'une association monospécifique à *Coeloenellina* indique des milieux semi-restrints et la présence de Leperditicopida, mise en évidence dans un échantillon étudié lors de l'analyse sédimentologique, atteste de conditions lagunaires. Ces conditions environnementales semi-restrintes et lagunaires se généralisent ensuite dans la partie moyenne et supérieure de la Formation de Trois-Fontaines tel qu'on peut l'observer dans la carrière de Rancennes, aussi au Mont d'Haur (CASIER *et al.*, 2010).

La sédimentation témoigne de la transition d'un système de rampe silico-carbonatée à un système de plate-forme carbonatée restreinte caractérisée par des dépôts péritidaux de basse énergie et lagunaires, et affectée fréquemment par une exposition subaérienne. L'évolution générale de la sédimentation montre que le milieu devient peu profond, ce qui témoigne d'une baisse relative du niveau marin au passage de la Formation d'Hanonet à la Formation de Trois-Fontaines. La rampe est caractérisée par

des environnements de forte énergie qui détruisent la plupart des bioconstructions à stromatopores et coraux apparaissant alors sous forme d'accumulations de floatstones et rudstones formant un biostrome épais. Dans ce contexte de haute énergie, on observe des bancs à *Girvanella* et Issinélides.

La courbe de susceptibilité magnétique en champ faible placée face à la colonne lithologique révèle quatre séquences magnétiques. Les courbes de susceptibilité magnétique et de microfaciès sont modérément corrélées et sont essentiellement liées à l'évolution des environnements d'une rampe vers une plate-forme. Les valeurs de susceptibilité magnétique sont très faibles au cours de l'unité biostromale avant d'atteindre les plus fortes valeurs dans l'environnement de lagon restreint de la Formation de Trois-Fontaines. Une corrélation stratigraphique à haute résolution est proposée entre la coupe du Mont d'Haur et celle de Baileux, située à une distance de 40 km, où des fluctuations similaires de la susceptibilité magnétique sont reconnues malgré une épaisseur plus forte des sédiments dans la coupe de Baileux. Le signal de susceptibilité magnétique est fortement contrôlé par les minéraux ferromagnétiques *s.l.* ainsi que par une contribution moindre des grains paramagnétiques. Le coefficient normalisé de viscosité magnétique et la décroissance d'IRM montre les valeurs les plus élevées dans les sédiments du lagon de la Formation de Trois-Fontaines qui présentent également les valeurs les plus élevées de susceptibilité magnétique. Ces résultats indiquent la présence d'une quantité significative de grains de magnétite de granulométrie ultrafine très probablement formés au cours de la diagenèse.

La liste des ostracodes givétiens, figurés par COEN (1985) et récemment versés dans les collections du Département de Paléontologie de l'Institut royal des Sciences naturelles de Belgique, est reportée en annexe. Ces ostracodes ont reçu des nouveaux numéros d'inventaire.

**Mots-clés:** Ostracodes, Séimentologie, Paléoécologie, Susceptibilité magnétique, Givétien inférieur, Synclinorium de Dinant, Ardennes, France.

## Introduction

This paper forms part of the series on the Middle Devonian ostracods and their lithological context in the type region for the definition of the Givetian Stage (southern part of the Dinant Synclinorium, Ardennes Department, France). A first paper (CASIER *et al.*, 2010) has been devoted to the Trois-Fontaines Formation (=Fm)/Terres d'Haur Fm boundary exposed in the Rancennes Quarry. It is located along the western rampart of a historically entrenched military camp at the Mont d'Haur (Fig. 1). The paper reported a quite rich and diversified ostracod fauna indicative of marine, semi-restricted and lagoonal environmental conditions. The Rancennes Quarry completes the stratotype of the Terres d'Haur Fm located on the southeastern flank of the entrenched camp. In fact, the Trois-Fontaines Fm/Terres d'Haur Fm boundary and subsequently the very base of the latter do not outcrop in the stratotype (HUBERT, 2008).

This second paper deals with the Hanonet Fm/

Trois-Fontaines Fm boundary at the Mont d'Haur. The Trois-Fontaines Fm belongs to the Givet Group. The studied section (GPS: N 50°07'40.2"; E 04°49'29.7") is more or less perpendicular to the southwestern rampart at the Mont d'Haur (Fig. 1). The section exposes the last 11.5 m of the Hanonet Fm composed of decimeter-thick bioclastic limestone beds (packstones) relatively rich in brachiopods, solitary corals (rugosa), stromatoporoids and crinoids, and the first 13.2 m of the Trois-Fontaines Fm composed in its basal part of thicker limestone beds (floatstones and rudstones) rich in corals (tabulata), massive stromatoporoids and molluscs, overlain by homogeneous medium-thick beds of fenestral mudstones and wackestones.

The *hemiansatus* conodont Zone defining the base of the Givetian (SDS Meeting, Rennes, 1988; WALLISER *et al.*, 1995) has been recognized in the Hanonet Fm stratotype (La Couvinoise Quarry), near the top of the lower part of this formation (BULTYNCK & DEJONGHE, 2001), 42 meters below the base of the Givet Group (BULTYNCK & HOLLEVOET, 1999). At the Mont d'Haur, *Icriodus obliquimarginatus*, whose occurrence indicates a zone of the alternative *Icriodus* conodont zonation, has been found by BULTYNCK (1987) 4 meters below the base of the Givet Group but this author estimates that it is certainly not the earliest record for the type area. In other sections in the Dinant Synclinorium, BULTYNCK (*ibid*) notices that *I. obliquimarginatus* first occurs up to 18 meters below the base of the Givet Group. Thus the part of the Hanonet Fm exposed in the section studied herein might be Givetian in age.

The section has been studied recently also by HUBERT (2008) and a list of 25 collected ostracod species was reported by MILHAU (*in HUBERT et al.*, 2007). Ostracods from other Givetian sections at the Mont d'Haur were also reported by BECKER & BLESS (1974) and COEN (1985). For the list of ostracods identified by COEN see Annex 1 (ostracods printed in bold), and ERRERA *et al.* (1972) and BULTYNCK *et al.* (1991) for further information and complete bibliography on the Givetian of Mont d'Haur.

## Rock and facies analysis (A. PRÉAT)

The studied Hanonet Fm/Trois-Fontaines Fm boundary interval exposes nearly twenty meters of poorly bedded fine- to medium-grained bluish clayey bioclastic wackestones and packstones (lower part) which are overlain by massive reefal limestone beds (meter-thick floatstones and rudstones; middle part) and well-bedded

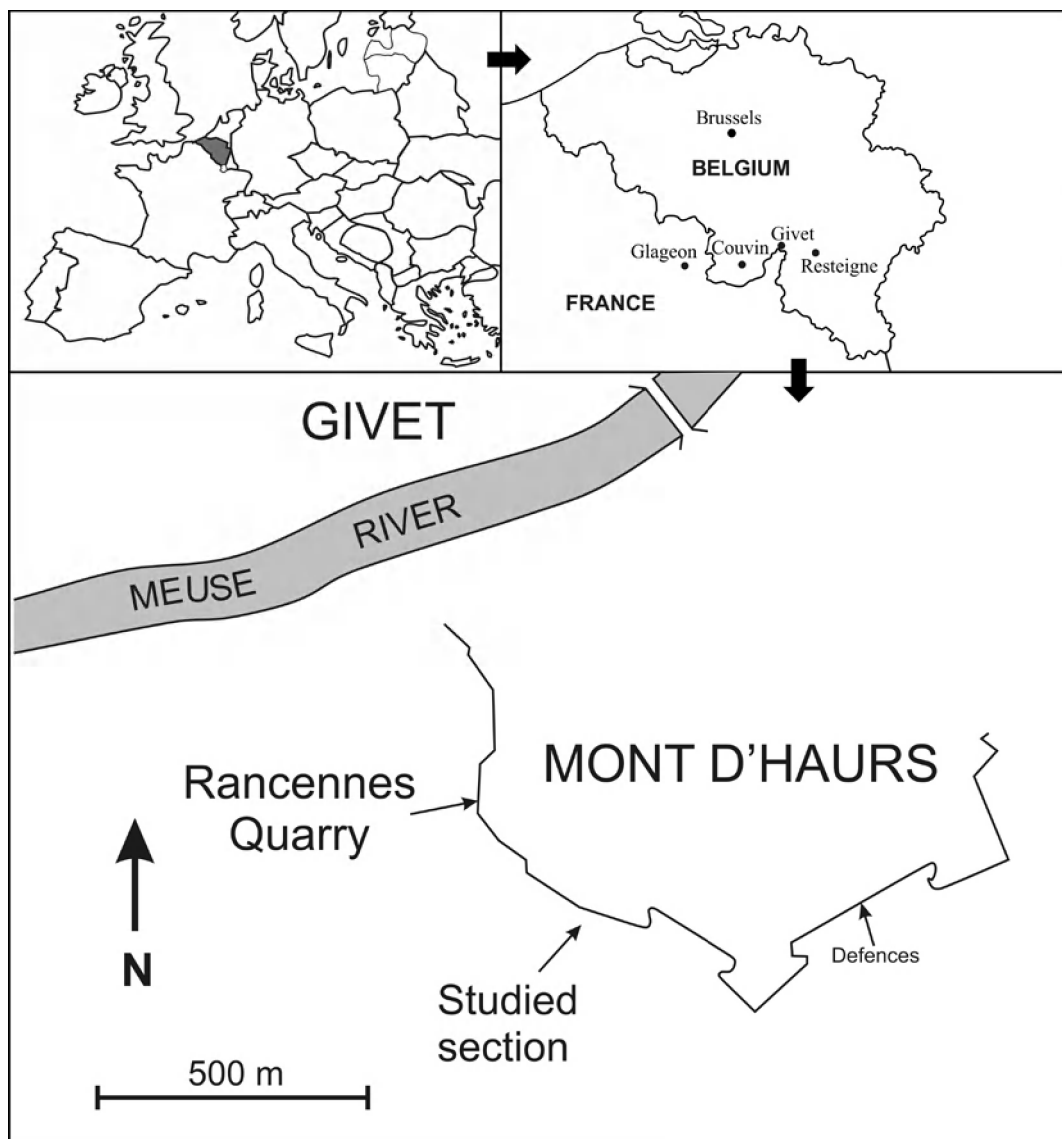


Fig. 1 – Location of the studied section and the Rancennes Quarry at the Mont d'Haurs.

greyish fine-grained mudstones and wackestones with abundant small-sized vertical fenestrae (upper part).

Crinoids (with preserved stems), solitary corals (rugosa) and various shell bioclasts are abundant in the lower part. The middle part consists of abundant broken massive stromatoporoids (with the size up to one meter), massive and fasciculate corals (rugosa and tabulata), crinoids, brachiopods and gastropods. The upper part is more homogeneous and gastropods are the only distinguishable fossils. The bedding of the series is regular. Fifty-eight samples (MH500-545 and MH600-612) have been collected (Fig. 2) for petrography in order to constrain the paleoenvironments. It is clear from the field observation that the three successive parts represent a pronounced sedimentological evolution from an open-marine environment towards a semi-

restricted or a restricted setting. The reefal part assuming the transition between these two environments is not in place as suggested by the reworking of organisms and consists of a biostrome. The large size of bioclasts (decimetre), their poor sorting and good preservation point to a short transport.

As the Hanonet Fm/Trois-Fontaines Fm boundary interval represents the transition from a mixed siliciclastic-carbonate ramp system to a carbonate platform in the Dinant Basin (KASIMI & PRÉAT, 1996), the microfacies distribution and evolution are rather complex, the key parameters for microfacies interpretation changed through time. PRÉAT & KASIMI (1995) proposed a standard sequence of ten major microfacies based on the energy index variation from open-marine (below the storm wave base level) to reefal

complexes, open lagoons and peritidal environments near emerged surface with vadose cavities. PRÉAT & MAMET (1989) developed a standard sequence of thirteen major microfacies types in the carbonate platform for the French-Belgian Givetian of the Dinant Basin and correlated them with the equivalent microfacies of the standard microfacies (SMF) *sensu* WILSON (1975). As the Givetian microfacies of the studied section are similar to the ones described in the above mentioned standard microfacies, we give their correspondent using the PRÉAT & KASIMI (1995) and PRÉAT & MAMET (1989) standard sequences as it has also been done for the Upper Givetian in CASIER *et al.* (2010). This way to proceed has the advantage to make easier comparison and discussion with the previous studies in the Devonian of the Dinant Basin. The lower and middle parts of the section consist only of open-marine facies of a ramp system, the upper part with true lagoonal deposits indicates a typical carbonate platform environment. Despite these two different sedimentary systems the standard sequences highlight a same shallowing-upward trend from subtidal open-marine environment near the storm-wave base level to supratidal settings with emerged surface.

### *Microfacies analysis*

#### *Microfacies type 1 (MF1)*

##### *Open-marine below storm-wave base*

This microfacies is not well represented and has not been sampled due to its relatively important clay content. It occurs in the lower part of the first interval and consists of centimetric or decimetric homogeneous clayey silty mudstones. This microfacies is equivalent to MF1 of PRÉAT & KASIMI (1995).

#### *Microfacies type 2 (MF2)*

##### *Open-marine environment near storm-wave base (Pl. 4, Figs 1, 2)*

*Description:* burrowed bioclastic and microbioclastic clayey and silty wackestones (Pl. 4, Fig. 2). The fine-grained bioclasts mostly consist of echinoderms (crinoids and sea urchin spines and plates), brachiopods, bryozoa, ostracods and very small-sized *Girvanella* fragments. A few larger bioclasts (*Girvanella*-encrusted crinoids and brachiopods) occur in thin (millimetre-thick) layers. Lamination is partly destroyed by bioturbation. Filamentous pyrite (*sensu* MAMET & PRÉAT, 2009) was observed inside bioclasts, mostly in the echinoderm plates (Pl. 4, Fig. 2). Irregular pressure solution seams are common and with accumulated pyrite (Pl. 4, Fig. 2).

*Interpretation:* the character and well-preserved bioclasts suggest a quiet open-marine environment, episodically interrupted by storm events as indicated by the occurrence of thin bioclastic layers (less than one millimetre-thick) which were not bioturbated. The *Girvanella* fragments point to the proximity of the euphotic zone. The environment could be compared with the transition zone described in the North Sea (German Bay) by AIGNER (1985). This microfacies is equivalent to MF2 of PRÉAT & KASIMI (1995).

#### *Microfacies type 3 (MF3)*

##### *Open-marine environment near storm-wave base, proximity of *Girvanella*-cyanobacterial mats (Pl. 4, Figs 3-6)*

*Description:* burrowed wackestones and peloidal packstones with abundant diversified medium- to coarse-grained bioclasts (brachiopods, bryozoa, ostracods, molluses, echinoderms). *Girvanella* are common as fragments (Pl. 4, Fig. 5), encrustations of bioclasts (Pl. 4, Figs 4, 6) or around nuclei of various oncrites (Pl. 4, Fig. 3). Peloids are irregular, well rounded and a few of them are reworked. *Girvanella*, *Rectangulina* ANTROPOV, 1959 are rare and occur as coarse-grained fragments. Coarser clasts and all bioclasts are concentrated in the interstratified thin (a few millimetres) packstone layers with a microspar matrix.

*Interpretation:* the abundance of the cyanobacterial or *Girvanella* fragments points to the proximity of a shoal colonized by microbial mats in the photic zone. The bioclastic packstone layers and the occurrence of coarse-grained bioclasts point to an environment exposed to episodic storms, which mixed several biocenoses (*Girvanella*, brachiopods etc.) in a general shallow-water open-marine setting. These layers are comparable to intermediate and proximal tempestites described by AIGNER (1985). This microfacies has no precise equivalent in the standard sequence of PRÉAT & KASIMI (1995) but might be similar to their MF3a with *Girvanella* replacing paleosiphonoclades.

#### *Microfacies type 4 (MF4)*

##### *Open-marine fore-reef environment around the fair-weather wave base (Pl. 4, Figs 7, 8)*

*Description:* crinoidal grainstones and bioclastic floatstones/rudstones with abundant coarse decimetre-(field observation) to centimetre-sized stromatoporoids and corals (mainly rugosa) subangular to subrounded fragments. Other bioclasts consist of brachiopods, molluses, bryozoa, ostracods and issinellids (algae). They are well preserved and often unbroken. Peloids

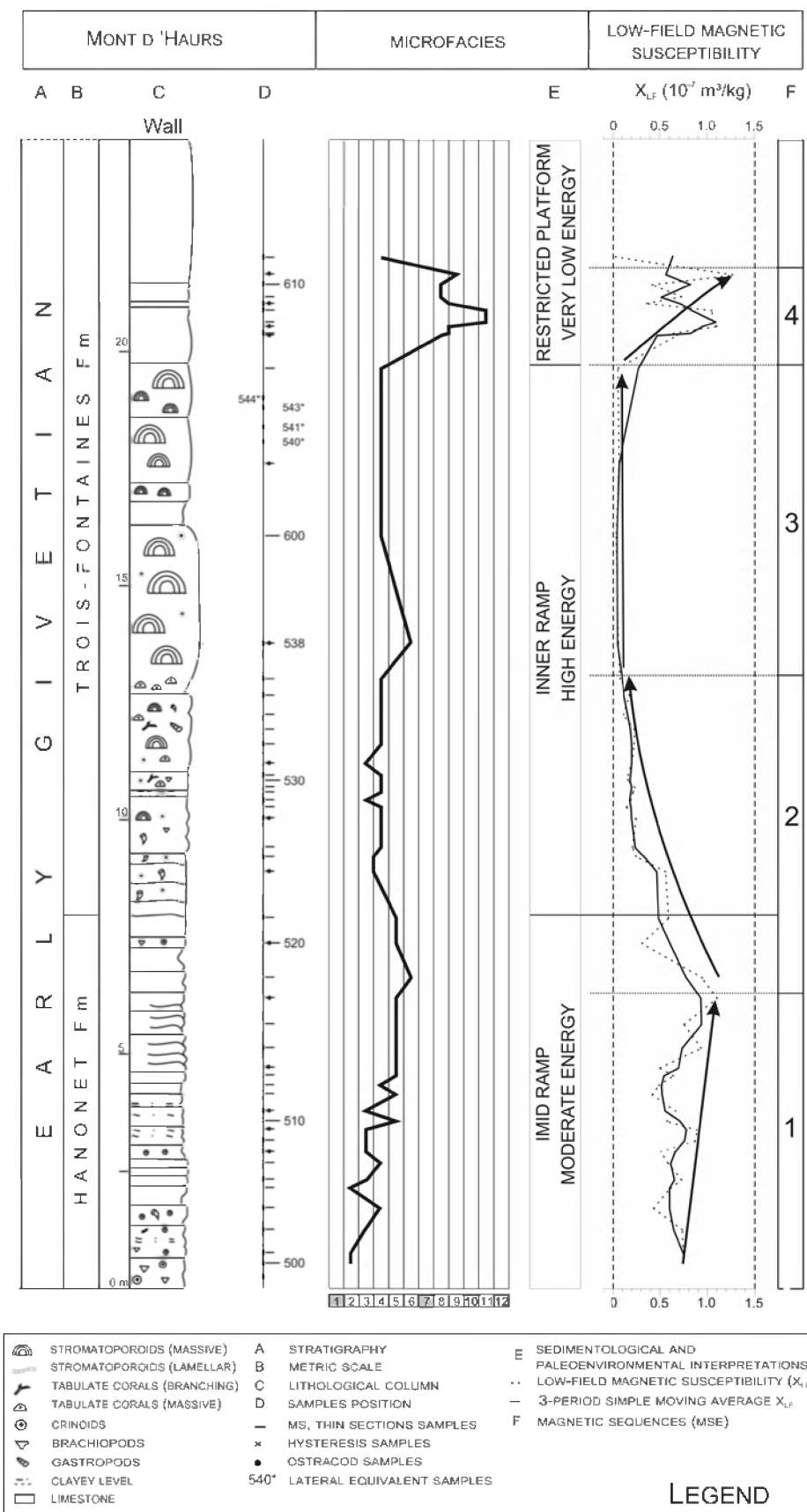


Fig. 2 – Lithological column of the Mont d'Haurs section with microfacies, paleoenvironmental interpretations and low-field MS curve divided into four magnetic sequences.

of *Girvanella* are common and very rare fragments of *Paralitania* MAMET & PRÉAT, 1985 have been observed. The stromatoporoids and corals show numerous encrustations. Graded bedding occurs as oblique bedding. In this case the bioclasts are not micritized and occur as relatively thick-bedded (0.5 – 5 mm) packstone layers. This is particularly true for the echinoderms that are well preserved and “fresh” (without microborings, not perforated, not micritized). In comparison with previous microfacies types, layers are thicker (up to a few centimetres), more abundant and with truncated bases. Sediment is slightly bioturbated and it can highlight a bimodal size-distribution of the grains by mixing of the grains of thick-bedded layers with those included in the matrix. The micritic matrix can be dolomitized but most of the bioclasts not. The syntaxial cement is mostly well-developed in crinoidal grainstones.

*Interpretation:* the abundance (field and thin section observations) of reworked stromatoporoids and corals mixed with echinoderms and brachiopods points to a fore-reef environment close or in the photic zone as suggested by presence of the issinellids, *Girvanella* and *Paralitania*. The abundance of the issinellids indicates that they were derived from a proximal shoal (MAMET & ROUX, 1981). This general high-energy reefal environment was exposed to episodic storms, which deposited thick-bedded packstone layers in the floatstones and rudstones. The grain size distribution of the bioclasts and layer thicknesses point to proximal tempestites *sensu* AIGNER (1985). The crinoidal grainstone microfacies is equivalent to the MF4 of PRÉAT & KASIMI (1995) and the reefal microfacies to MF5a or to MF5 of PRÉAT & MAMET (1989).

#### *Microfacies type 5 (MF5)*

*Open-marine fore-shoal environment around the fair-weather wave base (Pl. 5, Figs 1, 2)*

*Description:* fine-grained laminar bioclastic-peloidal packstones and grainstones with alternated with thick-bedded (below one centimetre) bioclastic layers (Pl. 5, Fig. 1). Despite the fact that the silt content is low (< 5 %) it constitutes a characteristic of the microfacies. As before, the *Girvanella* peloids dominate and consist of small-sized fragments. Larger fragments of *Girvanella* also occur. Bioclasts are well-sorted and consist mostly of echinoderms (crinoids) with a few molluscs (gastropods), brachiopods, ostracods and rare corals (rugosa) and tentaculitids. Cross-bedding and erosive discontinuities are present. Small-sized tentaculitid-like bioclasts are abundant. Rare *Bisphaera* BIRINA, 1948 (enigmatic taxon) appear in this microfacies (Pl.

5, Fig. 2). Micritized grains are not very abundant. Bioturbation is common.

*Interpretation:* well-sorted crinoid fragments derived from meadows dominate together with small-sized peloids probably derived from *Girvanella* mats or shoals. The energy was high (planar and oblique lamination, intercalations of thicker layers) and destroyed crinoidal meadows and *Girvanella* shoals or banks (HORBURY & ADAMS, 1996), fragments were recycled near the fair-weather wave base and then exported off the shore. Then the sediment was burrowed and most of the texture features (e.g. lamination etc.) were destroyed. This microfacies has no equivalent in the PRÉAT & MAMET (1989) or PRÉAT & KASIMI (1995) standard sequences. A similar microfacies has been defined near the Devonian-Carboniferous boundary in the northeastern part of the Dinant Basin (MF4 in CASIER *et al.*, 2005).

#### *Microfacies type 6 (MF6)*

*Semi-restricted back-reefal environment with moderate energy*

*Description:* stromatoporoid and coral (tabulata and rugosa) floatstones with abundant bioclasts, peloids and lumps (ranging from 50 to 500 µm) and rare protocoilites. Bioclasts are partly micritized and consist of brachiopods, pelecypods (mud-coated grains), large gastropods, abundant ostracods (disarticulated valves), echinoderms, issinellids, calcispheres and rare kamaenids. Stromatoporoids and corals are often encrusted. Bioturbation is not very abundant. Irregular small- and large-sized fenestrae occur giving to the rock the appearance of a loferite. The fenestrae are filled with thin fibrous calcite cement and a large granular sparite. The fenestrae are limited by small-sized peloids forming an irregular network (bacterial peloids? *sensu* MAMET & PRÉAT, 2005). The matrix can be partly replaced by fine-grained hypidiotopic and idiotopic dolomite (50 µm) and the fenestrae by saddle dolomite (up to 3 mm). The matrix is also partly recrystallized to fine-grained calcite microspar.

*Interpretation:* bioclasts consist of mixed open-marine and lagoonal (see below) organisms near a buildup dominated by stromatoporoids and corals. The fenestral fabric and the mud-coated grains point to a shallow subtidal and intertidal environment (SHINN, 1983) in a general back-reefal setting indicated by the occurrence of the constructors, and calcispheres and kamaenids pointing to a semi-restricted or restricted domain. Absence of microbreccias points to a moderate energy not so strong enough to break the bioclasts. This microfacies is similar to MF6 in PRÉAT & MAMET (1989) and MF7 in PRÉAT & KASIMI (1995).

***Microfacies type 7 (MF7)***

Microfacies type 7 *sensu* PRÉAT & MAMET (1989) was not found as well as in PRÉAT & KASIMI (1995).

***Microfacies type 8 (MF8)***

*Restricted environments with salinity fluctuations* (Pl. 5, Figs 1, 2)

*Description:* wackestones with centimetre-thick coarse bioclastic (gastropods, pelecypods, tabulata, stromatoporoids) layers in fenestral peloidal wackestones-packstones with abundant calcispheres. The matrix is micritic and contains kamaenids, labyrinthoconids (LANGER, 1979), *Bisphaera*, nodules of *Bevocastria* (GARWOOD, 1931) and ostracods. Most of the peloids comes from *Bevocastria*. The fenestrae are irregular (*sensu* TEBBUTT *et al.*, 1965; SHINN, 1968, 1983) in millimetre scale with rare geopetal infillings (very often dissolved gastropods). However, true irregular fenestrae occur but they do not dominate. *Bevocastria* intensively encrusts large bioclases (mostly corals and stromatoporoids) forming irregular oncoids and transforming the sediment in a bindstone. Medium-sized calcite microspar form the packstone matrix whereas micrite the wackestone matrix. The bioturbation occurs and destroys the texture of bioclastic layers.

*Interpretation:* microflora, cyanobacteria or “cryptalgae” (*Bevocastria*) and calcispheres dominate and point to a restricted lagoon (PRÉAT & MAMET, 1989). Open-marine fauna is absent, except for the load of redeposited fauna during the episodic storms. The environment is isolated from the offshore and very quiet. The gastropod accumulations in thick layers are products of littoral or tidal current activity in this very shallow setting (WAGNER & VAN DER TOGT, 1973; ENOS, 1983). This microfacies is equivalent to the MF8 of PRÉAT & MAMET (1989).

***Microfacies type 9 (MF9)* (Pl. 5, Figs 5, 7)**

*Description:* homogeneous mudstones and peloidal wackestones with abundant calcispheres and Leperditicopida. The matrix contains kamaenids, proninellids, labyrinthoconids, *Bevocastria*, sponge spicules, amphiporids and large bipyramidal quartz grains (width of 30 µm and length of 150 µm). Large- and small-sized irregular fenestrae are abundant and the sediment looks like a loferite. The bipyramidal quartz grains are sometimes very abundant with tiny sulphate? inclusions and replace laths of former mineral which display also a swallow-tail habitus. Bioturbation is not developed. The matrix contains abundant frambooidal pyrite. A few fenestrae exhibit

a well-rounded morphology and might be related to primary evaporite nodules (GUILLEVIN, 1979). As in the previous microfacies a coarse saddle dolomite occurs in some fenestrae.

*Interpretation:* microflora and microfauna are the same as in the previous microfacies and point to a very quiet and restricted lagoon. The environment was very shallow as suggested by the occurrence of fenestral fabric. Salinity oscillations are indicated by the endemism of organisms, i.e., Leperditicopida (brackish water), amphiporids and probable pseudomorphs after sulphate nodules (from hypersaline brines). The algal associations and the development of *Bevocastria* indicate stressfull conditions. This microfacies is equivalent to the MF9 of PRÉAT & MAMET (1989), this microfacies is the most typical for the Givetian of the Dinant Basin in Belgium and France.

***Microfacies type 10 (MF10)***

Microfacies type 10 *sensu* PRÉAT & MAMET (1989) was not observed as in PRÉAT & KASIMI (1995).

***Microfacies type 11 (MF11)***

*Description:* homogeneous dolomudstone with a few calcispheres, ostracods and rare labyrinthoconids with a very well developed fenestral fabric. Irregular fenestrae have geopetal infillings with crystal silt overlying or mixed with peloidal layers. Sparite fills the upper part of the fenestrae or cavities. Spar-micrite *sensu* KAHLE (1977) occurs in the matrix and consists of a heterogeneous recrystallized dolomicrosparite with residues of micrite and peloids. The microfacies is quite similar to MF11 of PRÉAT & MAMET (1989) or to MF11 and MF12 of the standard sequence of the Viséan of Northern France (MAMET & PRÉAT, 2005).

*Interpretation:* very low diversity of the organisms suggests significantly stressfull environment with possible emerging as indicated by the geopetal fillings of the fenestrae. Alteration of micritic matrix through micritisation processes of organisms points to the proximity of the vadose zone or emerged surface where soils can develop.

***Microfacies types 12 and 13***

Microfacies types 12 and 13 *sensu* PRÉAT & MAMET (1989) were not observed in the studied section.

***Microfacies and evolution of sedimentary setting***

The first six microfacies consisting of mudstones, wackestones, packstones, grainstones and floatstones or rudstones are dependent on the energy of the

sedimentation regime. The laminae and thicker bioclastic layers record the relative bathymetry of the storm- and the fair-weather wave bases (AHR, 1973; EINSELE & SEILACHER, 1982). Laminar intervals, which are rare and thin-bedded in MF2, thicker in MF3 than in MF2, thickest and abundant in MF5, are composed of similar bioclasts. The bioclast size increases with lamination thickness and with the diversity of the faunal assemblages, particularly when fragments of fossils occur. Cross bedding is an abundant feature in MF5 and the rate of bioturbation significantly decreases. The occurrence of *Girvanella* across all these microfacies indicates a depositional environment within the euphotic zone in an open-marine domain in shallow water as also indicated by faunal assemblages (echinoderms, brachiopods, bryozoa). Generally, the background sedimentation is decantation of clay components and carbonate muds from water column, in a quiet environment (MF1). MF2 and MF3 were gradually affected by storm activities, which caused the increased flux of coarse bioclasts. Intermittent energy allowed development of *Girvanella* oncoids (MF3). Oscillation in the energy was very high near the fair-weather base level and laminar crinoidal grainstones/rudstones (MF4) or *Girvanella* peloidal packstones/grainstones (MF5) were deposited in the shoals. The rate of bioturbation decreased probably due to the high sedimentation rate and increased erosion (erosional laminations, cross-bedding, good sorting of material). In such conditions, crinoidal meadows and “cryptalgal” or cyanobacterial (*Girvanella*) mats on shoals were episodically destroyed and exported to MF2 and MF3. However the energy was not so high and thus no microbreccias developed. Material was cemented early. Massive rugosa, massive and branched tabulata and massive (decimeter up to meter) stromatoporoids are abundant in MF6 and indicate the presence of a buildup. The shallow-water material was transported to the offshore domain (MF4) or to semi-restricted environments where they were mixed with typical lagoonal flora and fauna (MF9). Neither true framestones as those of the “Fondry des Chiens” at Nismes (PRÉAT *et al.*, 2007; MAMET & PRÉAT, 2009) or of Wellin at the south border of the Dinant basin (MAMET & PRÉAT, 2005) were identified, nor early thick fibrous cements on bioclasts. MF4 and MF6 are equivalent to the microfacies of the first biostrome of the Trois-Fontaines Fm (COEN-AUBERT *et al.*, 1986), which formed a marker bed along the southern border of the Dinant Basin. It probably corresponds to the destruction of bioherms similar to those of Nismes and Wellin. The restricted environment was dominated by

nodular cyanophyceans (*Bevocastria*) and calcispheres in subtidal zones (MF9) and by loferites in intertidal and supratidal domains (MF11). The sedimentation was limited to the protected lagoon isolated from the open-marine circulation except during episodic storms, which caused the accumulation of thick gastropod shells (MF8).

The general evolution of the sedimentary environment is characterized by the shift from open-marine environment (below storm-wave base) to a reefal complex (“first biostrome”), open lagoons and peritidal environments near an emerged land. The sedimentary model consists of a siliciclastic carbonate mid-inner ramp setting (*sensu* AHR, 1973) developed into a carbonate platform (*sensu* PRÉAT & MAMET, 1989) due to a gradual relative sea-level fall (PRÉAT *et al.*, 2007; MAMET & PRÉAT, 2009).

The key parameter driving this evolution was a general increase in the energy, which accompanied the relative sea-level fall. The energy was constantly too high for the preservation of elementary parasequences (5<sup>th</sup> order *sensu* VAN WAGONER *et al.*, 1987; VAIL *et al.*, 1991). For the same reason no evident parasequence set pattern (4<sup>th</sup> order, *ibid.*) appears. The only elementary parasequence identified is associated with the first development of the true carbonate platform setting. This parasequence is plurimetric-thick and records a subtidal/supratidal shallowing-up evolution of the sedimentary environment. This parasequence is the first one in the studied succession and probably precedes the numerous similar parasequences (“regressive rhythms” *sensu* PRÉAT & MAMET, 1989), which characterize the Trois-Fontaines Fm in the Lower Givetian of Belgium and Northern France.

## Magnetic Susceptibility (X. DEVLEESCHOUWER & E. PETITCLERC)

Whole-core MS logging of deep-sea sediments, mainly for high-resolution lithostratigraphic correlation, has become a routine procedure during Ocean Drilling Program (ODP) cruises since 1986 (BLOEMENDAL *et al.*, 1989). MS data were used mostly for the Quaternary sediments to identify glacial and interglacial sequences. During the nineties, MS studies were applied to older rocks such as the Devonian carbonates of the Tafilalt and Mader basins (CRICK *et al.*, 1994) and the Upper Devonian (Frasnian-Famennian boundary) in Europe (DEVLEESCHOUWER, 1999; DEVLEESCHOUWER *et al.*, 1999; RIQUIER *et al.*, 2010). The changes in the flux of detrital material coming into the sedimentary

environment represent important cause of the MS variations (ELLWOOD *et al.*, 2000), these are related to the changes in the terrigenous clastic material supply from the continent to the marine realm (CRICK *et al.*, 2001). It is generally explained by sea-level oscillations with high MS values during regressions where an increase of erosion on exposed continental masses can deliver more detrital minerals into the marine realm. On the contrary, low MS values are recorded during transgressive episodes (CRICK *et al.*, 1997, 2000, 2001). An increased detrital input to the marine domain will enhance the MS signal due to a higher abundance of grains of magnetic material. Different sources of non-carbonate (mostly terrigenous material) are related to riverine (CRICK *et al.*, 2000, 2001), volcanic activity (GORBARENKO *et al.*, 2002), hydrothermal vents (BORRADAILE & LAGROIX, 2000), bolide impacts (ELLWOOD *et al.*, 2003), eolian supply (HLADIL, 2002; HLADIL *et al.*, 2006) and products of pedogenesis during the formation of paleosols (CHEN *et al.*, 2005).

MS logging is considered to be a very useful high-resolution stratigraphic tool with great potential for correlations of sedimentary sequences within the same basin in local scale or even between different basins in global scale (ELLWOOD *et al.*, 2001, 2007, 2008). The use of the MS logging for the Paleozoic sediments is meaningful only with a biostratigraphic control and the use of other techniques such as the microfacies.

### **Material and methods**

In this study, the same samples used for sedimentological analyses were sliced into rectangular parallelepiped rock pieces. The MS measurements were carried out at the Royal Belgian Institute of Natural Sciences using MFK1-A susceptometer at room temperature in a low AC magnetic field of 400 A/m and at a frequency of 976 Hz. The MS values of the samples were corrected for the susceptibility of the empty plastic holder. Each sample was weighted with a precision of 0.01 g, measured three times and the results averaged. A mass specific low-field MS ( $X_{LF}$ ) was calculated for each sample. The MS is dependent on the mineralogical composition of the rock and the amount of the mineral phases. It integrates the contribution of the different magnetic mineral fractions according to their dia-, para- or ferromagnetic *s.l.* behaviour. Any change in the composition, concentration and grain-size of the minerals is expressed in the  $X_{LF}$  value. This property enables using the  $X_{LF}$  measurements as a very sensitive proxy for the changes in the rock composition. In the

sedimentary rocks, MS logging records fluctuations in the amounts and contributions of diamagnetic (mostly quartz, calcite), paramagnetic (mostly clay minerals, pyrite and iron carbonates) or ferromagnetic *s.l.* phases (iron oxides and oxyhydroxides, iron-rich sulphides). Thus bed-by-bed  $X_{LF}$  logging through the section can display changes in the flux and/or sources of detrital input (ANDREWS & STRAVERS, 1993; ROBINSON, 1993; VANDERAVEROET *et al.*, 1999; ELLWOOD *et al.*, 2000). Hysteresis parameter measurements were carried out on sixteen samples selected on the entire MS measurements, microfacies types and sedimentological characteristics. The shape of a hysteresis curve is characteristic for each rock with different magnetic properties, and shows the ease of magnetising and the ability to retain the magnetisation (EVANS & HELLER, 2003). Isothermal magnetisation curves were performed at the Geophysical centre of the Royal Meteorological Institute using a J-Coercivity "rotation" magnetometer developed by Kazan University (BUROV *et al.*, 1986) for rectangular parallelepiped rock pieces placed in a small paper box. The magnetising field was increased every 0.5 mT from 0 to +500 mT, then decreased to zero and further decreased to -500 mT and induced and remanent magnetisations were measured at each field increase/decrease. Finally, the decay of the isothermal remanent magnetisation at 500 mT or  $IRM_{500mT}$  was monitored for about 100 s.

### **Magnetic Susceptibility curve**

The low-field MS values ranging between  $-2.42 \times 10^{-9}$  and  $1.28 \times 10^{-7} \text{ m}^3/\text{kg}$  (Fig. 2) are weak as usually observed in most of the carbonate rocks (between  $1 \times 10^{-9}$  and  $1 \times 10^{-7} \text{ m}^3/\text{kg}$ ; ELLWOOD *et al.*, 1999). The highest  $X_{LF}$  value ( $1.28 \times 10^{-7} \text{ m}^3/\text{kg}$ ) was measured in MF9 corresponding to a restricted lagoonal environment of the Trois-Fontaines Fm. Despite the low  $X_{LF}$  values, the MS signal varies along the lithological column with several MS evolutions (MSE) reported as magnetic sequences. Four main MSE, numbered MSE 1 to MSE 4, were identified (Fig. 2). MSE 1, beginning at the base of the section in the Hanonet Fm, displays a gradual increasing  $X_{LF}$  trend from  $0.75$  to  $1.12 \times 10^{-7} \text{ m}^3/\text{kg}$ . Two moderately elevated values ( $0.9 \times 10^{-7} \text{ m}^3/\text{kg}$ ) in the samples MH507 and MH508 occurred in the middle part of MSE 1. This first magnetic sequence can be correlated to the regressive evolution from a quiet open-marine environment in the storm-wave zone (MF2) to the open-marine fore-shoal environment close or within the fair-weather wave zone (MF5). MSE 2, characterised by decreasing  $X_{LF}$  values from

1.12 to  $0.056 \times 10^{-7} \text{ m}^3/\text{kg}$ , encompasses the boundary interval between the Hanonet and Trois-Fontaines formations. A transition from semi-restricted back-reef (MF6) at the base of MSE 2 to open-marine fore-reef environment (MF4) may represent a small transgressive pulse. Relatively stable conditions in the open-marine environment characterised by the microfacies MF3 and MF4 are mirrored in the second half of MSE 2. MSE 3 (defined by four samples) corresponds to the first biostrome of the Trois-Fontaines Fm. MSE 3 contains very low  $X_{LF}$  values (below  $0.11 \times 10^{-7} \text{ m}^3/\text{kg}$ ). Finally, MSE 4 shows significantly high-amplitude oscillations in the  $X_{LF}$  values (mean value:  $0.82 \times 10^{-7} \text{ m}^3/\text{kg}$ ) with several peaks (above  $1.0 \times 10^{-7} \text{ m}^3/\text{kg}$ ) observed in MF9 (restricted lagoonal environment) and MF11 (restricted lagoonal environment close to the emersion).

High MS values were also reported from the sediments of the Couvin Fm (Eifelian) in Unit 5 at the Eau-Noire section and in Unit B at the Villers-la-Tour section in Belgium (MABILLE *et al.*, 2007). For these authors, the upper part of the Couvin Fm in the Abîme Member consists of micritic mudstone and wackestone with calcispherids, ostracods and fenestrae (MF13) and well-sorted peloidal grainstones representing MF14. These microfacies are indicative of intertidal and restricted lagoonal conditions in a platform model with peaks in the MS (mean value:  $1.049 \times 10^{-7} \text{ m}^3/\text{kg}$ ) observed only in MF13 and related to a strong terrigenous influx (MABILLE *et al.*, 2007). It must be noticed that MF13 in the Eau-Noire section display MS values ranging between  $3.5$  and  $16 \times 10^{-8} \text{ m}^3/\text{kg}$ . In the Eau Noire and Villers-la-Tour sections, MF14 is characterised by very low MS values (mean value:  $9.25 \times 10^{-9} \text{ m}^3/\text{kg}$ ), which was interpreted by MABILLE *et al.* (2007) as a consequence of permanent wave agitation preventing the settling of fine detrital particles. Similar conclusions have been proposed for microfacies MFa11 (mean value:  $12.14 \times 10^{-8} \text{ m}^3/\text{kg}$ ) and MFa12 (mean value:  $3.94 \times 10^{-8} \text{ m}^3/\text{kg}$ ) of the lagoonal sediments of the Trois-Fontaines Fm at the Baileux section (MABILLE & BOULVAIN, 2008). These interpretations were based only on sedimentological characteristics without any information on the type or grain-size of the magnetic minerals carrying the  $X_{LF}$  signal. MF13 in the Couvin Fm platform model corresponds to MF9 and MF11 defined here in the Mont d'Haur section. Restricted and intertidal lagoonal sediments are thus characterized by very strong  $X_{LF}$  values, which must be studied more in detail to identify the magnetic minerals and their grain-size distribution.

A drop in the  $X_{LF}$  values was observed in the last sample of the Mont d'Haur section (lowest value:

$-2.42 \times 10^{-9} \text{ m}^3/\text{kg}$ ) and it might represent a base of another MSE. This last MSE is only outlined here because it would be based only on one sample. This strong decreasing trend indicates the return to open-marine fore-reef environment (MF4).

### Comparison of microfacies and $X_{LF}$ curves

The  $X_{LF}$  and microfacies logs show a generally good correlative pattern along the Mont d'Haur section (Fig. 2). There is only one exception at the base of MSE 3 where the  $X_{LF}$  values are weak without any fluctuations and do not follow the change from MF4 to MF6 observed in the microfacies. The mean  $X_{LF}$  values with their standard deviations are plotted against microfacies (Fig. 3). The number of samples ( $n$ ) is also added to each microfacies. A linear regression between  $X_{LF}$  and microfacies (line with black triangles, Fig. 3) shows the coefficient of determination  $R^2=0.44$  (indicating that 44% of the variability in the data is explained by this model). The correlation coefficient  $r=0.66$  indicates a moderately positive correlation between these two parameters. The average  $X_{LF}$  value decreases from  $0.68 \times 10^{-7} \text{ m}^3/\text{kg}$  for MF2 to  $0.198 \times 10^{-7} \text{ m}^3/\text{kg}$  for MF4 in the open-marine environment. The average  $X_{LF}$  value of MF5 is higher ( $0.644 \times 10^{-7} \text{ m}^3/\text{kg}$ ) and corresponds to the fore-shoal environment close to the fair-weather-wave base. A progressive increase in the average  $X_{LF}$  value is then observed from back-reef MF6 (mean value:  $0.48 \times 10^{-7} \text{ m}^3/\text{kg}$ ) to restricted lagoonal environment close to the emerged surface or MF11 (mean value:  $1.066 \times 10^{-7} \text{ m}^3/\text{kg}$ ).

These microfacies correspond to the mixing between the microfacies standard sequence (MF1 – MF10 sensu PRÉAT & KASIMI, 1995) of the Eifelian-Givetian boundary interval mixed siliciclastic-carbonate ramp and the microfacies standard sequence (MF1 – MF12 sensu PRÉAT & MAMET, 1989) of the Givetian carbonate platform. Following these two standard sequences, the section could be subdivided into two sequences. The microfacies MF1 to MF6 of the Hanonet Fm and the base of the Trois-Fontaines Fm have a very weak linear correlation (dashed line with black squares, Fig. 3) with the square of the correlation coefficient  $R^2=0.07$ , which means that 7 % of the variability in the data are explained by this model. This result implies a correlation coefficient ( $r=0.26$ ) indicating a very weak positive correlation. This is indicative that there is no clear link between the microfacies and the  $X_{LF}$  values. On the contrary, a linear regression (dashed line with black circles, Fig. 3) calculated for the average  $X_{LF}$  values for MF8, MF9 and MF11 in restricted lagoonal

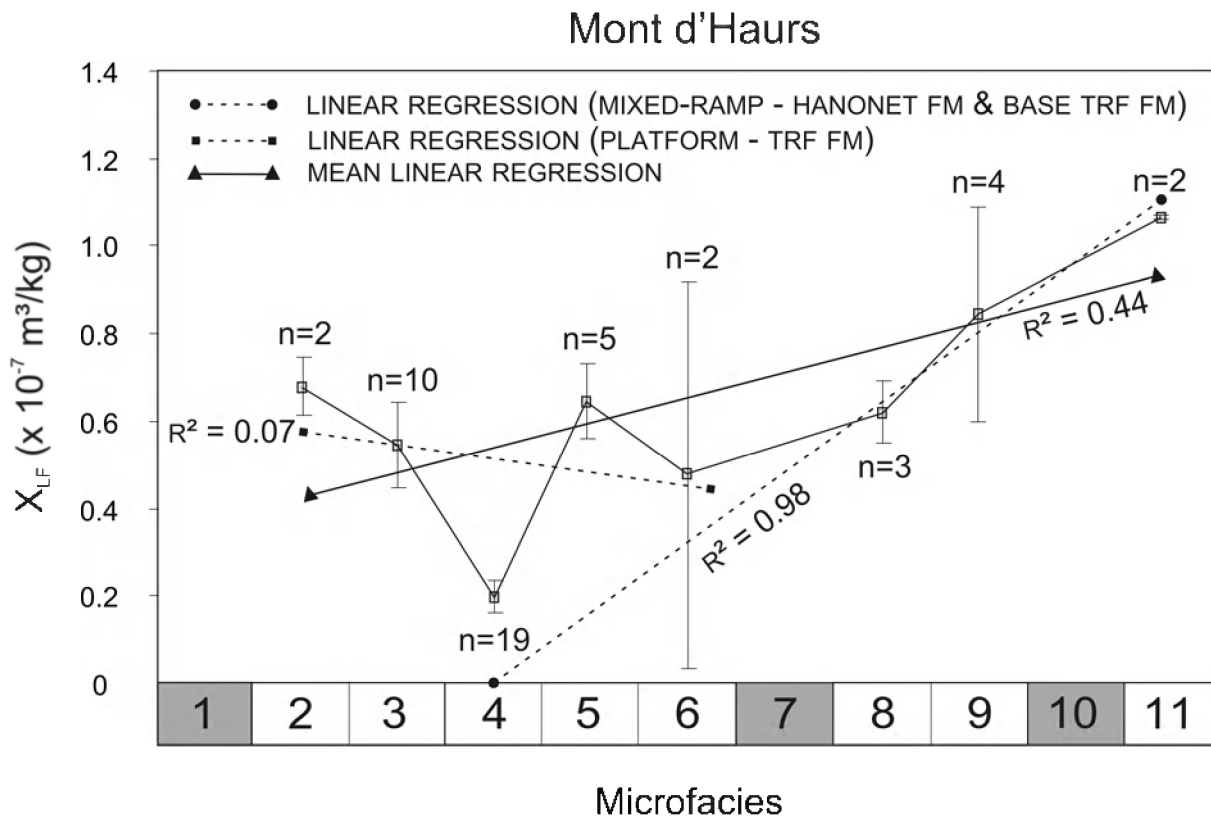


Fig. 3 – The mean low-field MS values plotted against microfacies in the Mont d'Haur's section. Three linear regression lines and models are figured: black line with black triangles represents the model for the whole section; dashed line with black squares represents the microfacies in the ramp setting whereas the dashed line with black circles represents the microfacies of the carbonate platform setting of the Trois-Fontaines Formation. The coefficient of determination  $R^2$  is assigned to each linear regression model.

environment and the last sample ( $X_{LF}$  value:  $-2.42 \times 10^{-9} \text{ m}^3/\text{kg}$ ), representing a fore-reef environment (MF4), reached a very high squared correlation coefficient ( $R^2=0.98$ ). This last linear regression model has a correlation coefficient ( $r=0.99$ ) representing a very strong positive correlation between the microfacies and the  $X_{LF}$ . To sum up, these results demonstrate a strong positive correlation between microfacies and  $X_{LF}$  values in the lagoonal facies in the carbonate platform of the Trois-Fontaines Fm and the very weak and anti-correlated link between the microfacies (MF1 to MF6) and the  $X_{LF}$  values in the mixed siliciclastic-carbonate ramp of the Hanonet Fm.

The MS is probably strongly influenced by the depositional profile, lithogenic input, sedimentation rate and water agitation during deposition and diagenesis (DA SILVA *et al.*, 2009). These authors have presented microfacies and depositional profiles of the Eifelian-Givetian boundary interval in a mixed ramp (Hanonet Fm, La Couvinoise section) and distal platform (Hanonet Fm, Baileux section) settings. These sections

are characterised by different average MS values along a distal-proximal profiles: 1°) the mixed ramp has much more higher values in the outer part compared to the low MS values in the middle and inner part of the ramp, 2°) the platform has the highest MS values in the lagoonal floatstone facies with branching corals (microfacies b7, DA SILVA *et al.*, 2009). The average  $X_{LF}$  value along the distal-proximal profile of the Mont d'Haur's section cannot be easily compared to these two other profiles. The  $X_{LF}$  values of the Mont d'Haur's section are more or less similar to those of the outer and mid-ramp environments of the La Couvinoise section. However, the average  $X_{LF}$  values are much higher here in the mid-ramp facies (MF5;  $6.44 \times 10^{-8} \text{ m}^3/\text{kg}$ ) underlined by a high peak in the profile instead of gradual increasing trend in the mid-inner ramp facies ranging from  $2.6$  to  $4.8 \times 10^{-8} \text{ m}^3/\text{kg}$  like in the La Couvinoise section (DA SILVA *et al.*, 2009).

For the microfacies observed in restricted lagoonal environment of the internal carbonate platform of the Trois-Fontaines Fm at the Mont d'Haur's section, high

average  $X_{LF}$  values characterise the microfacies MF8, MF9 and MF11 indicating a gradual increase from 6.11 to  $10.66 \times 10^{-8} \text{ m}^3/\text{kg}$ . These data seem to be similar to the average MS values along the distal-proximal profile characteristic for the lagoonal microfacies a4-a6 of the internal part of the Frasnian carbonate platform (DA SILVA *et al.*, 2009). It is obviously different from the microfacies b5, b6 and b8 described in the internal part of the Eifelian-Givetian boundary interval platform (Baileux section), which are characterised by low MS values (below  $4.0 \times 10^{-8} \text{ m}^3/\text{kg}$ ) and from microfacies b7, floatstone with branching corals, representing an abrupt rise to  $9.3 \times 10^{-8} \text{ m}^3/\text{kg}$  (DA SILVA *et al.*, 2009). Evidently, the Mont d'Haurs section data presented here reveals higher  $X_{LF}$  values and a stronger linear increasing trend along the microfacies of the Trois-Fontaines lagoonal environment compared to those of the Frasnian platform.

The Hanonet Fm and Trois-Fontaines Fm of the Baileux section have a thickness respectively of 95 and 91 meters (MABILLE & BOULVAIN, 2008). The authors subdivided these 186 meters into 9 magnetic susceptibility evolutions. Based on the range of the  $X_{LF}$  values and the evolution of the MS log, the magnetic sequences three to seven in the Baileux section could be correlated to all the magnetic sequence described here in the Mont d'Haurs section (MSE 1 to MSE 4). Surprisingly, the measured thickness for the Mont d'Haurs section corresponds to 24.7 meters, which could correspond to 113 meters in the Baileux section for the same stratigraphic interval. If this postulate is correct, a high-resolution stratigraphic correlation is thus proposed for the Mont d'Haurs section and the 40 km-distant Baileux section. The thickness difference corresponds mostly to the base of the Trois-Fontaines Fm in the Baileux section where the crinoidal sole, the biostromal unit and the base of the lagoonal unit are thicker, pointing out important lateral variations within the Trois-Fontaines Fm.

### **Magnetic mineralogy**

The  $X_{LF}$  data were coupled to twenty-four magnetic hysteresis measurements to identify the magnetic minerals carrying the  $X_{LF}$  signal and their grain-size. Hysteresis parameters, calculated from the hysteresis curves, indicate that the MS signal is strongly controlled by ferromagnetic *s.l.* minerals (i.e. a mixture of magnetite and a significant contribution of a high-coercivity phase, which might be hematite or goethite) with a minor contribution of paramagnetic grains. The  $X_{LF}$  curve is also controlled by the ferromagnetic *s.l.*

grains in the limestones at the top of the Fromelennes Fm close to the Givetian-Frasnian boundary in the Nismes section, Belgium (DEVLEESCHOUWER *et al.*, 2010). The transition from the mixed mid- to inner ramp environment to the restricted lagoon in the carbonate platform is accompanied by a sea-level fall and an input of coarse-grained ferromagnetic *s.l.* minerals (probably of detrital origin).

In general, 6.11 to 16.60 % of the  $\text{IRM}_{500\text{mT}}$  lost within one hundred seconds indicate the occurrence of superparamagnetic and/or viscous grains, which might be rather of diagenetic than of detrital origin. The IRM loss is higher in the lagoonal sediments (mean value of 13.73 %) compared to the base of the section in the open-marine mid-ramp environment (mean value of 8.96 %). The normalized magnetic viscosity coefficient ( $S_d$ ) shows an increasing trend from a mean value of 0.03 at the base of the section towards the highest value of 0.45 in the lagoonal sediments of the Trois-Fontaines Fm at the top of the section where the  $X_{LF}$  values are also the strongest. This increasing trend of the  $S_d$  and IRM loss parameter characterizes the whole section. These results seem to correlate with a significant abundance of ultrafine-grained grains, probably of magnetite type, close to the superparamagnetic (SP) / single domain (SD) grain-size (commonly accepted boundary size of 30 nm; DUNLOP, 2002) as already reported from the limestones of the Fromelennes Fm (DEVLEESCHOUWER *et al.*, 2010) and the Devonian platform carbonates of the Rhenish massif (ZWING *et al.*, 2005). The neoformation of large SP magnetite grains most likely as a by-product during the conversion of smectite into illite is proposed for the Devonian remagnetized limestones in the Ardennes fold-and-thrust belt (ZEGERS *et al.*, 2003). The occurrence of authigenic magnetite SP grains as a product of a chemical remanent magnetization (CRM) process clearly indicates that diagenesis has affected and modified the magnetic signature of these carbonates after deposition.

### **Ostracods (J.-G. CASIER)**

### **Material and methods**

Twenty-six samples of about 500 g each were collected in the section. All samples were crushed by a hydraulic press and about 100 g of each samples was processed using 99.8% glacial acetic acid, at nearly 90 °C, for four days at a rate of eight hours a day. This mode of extraction, called hot acetolysis method, was described by LETHIERS & CRASQUIN-SOLEAU (1988).

The residues were sieved on 250 µm and 1600 µm mesh screens. The process was repeated two times for the majority of samples, and three times for samples MH-499, 523, 525, 531, 533, 538, 543, 604, 608, 610 and 612. Approximatively 870 carapaces, valves and fragments of ostracods identifiable at any taxonomic level were thus extracted from the Hanonet Fm and Trois-Fontaines Fm. The stratigraphic position of the collected ostracods is shown in the Fig. 2.

### *Systematic position of the ostracod species*

ORDER LEPERDITICOPIDA SCOTT, 1961  
Leperditicopida indet.

ORDER PALAEOCOPIDA HENNINGSMOEN, 1953  
Suborder Palaeocopina HENNINGSMOEN, 1953  
Superfamily Kirkbyoidea ULRICH & BASSLER, 1906  
Family Amphissitidae KNIGHT, 1928  
*Amphissites tener omphalotus* BECKER, 1964  
Pl. 1, Fig. 1

Superfamily Hollinoidea SWARTZ, 1936  
Famille Hollinidae SWARTZ, 1936  
*Parabolbinella coeni* nov. sp.  
Fig. 4 in text, Pl. 1, Fig. 2,

Superfamily Beyrichioidea MATTHEW, 1886  
Family Beyrichidae MATTHEW, 1886  
*Kozlowskiella* sp. C in CASIER et al. (1994)  
Pl. 1, Fig. 3

Superfamily Aparachitoidea JONES, 1901  
Family Aparachitidae JONES, 1901  
*Aparchites* sp. A in CASIER et al. (2010)  
Pl. 1, Fig. 7

Family Rozhdestvenskayitidae MC GILL, 1966  
*Fellerites crumena* (KUMMEROW, 1953)  
Pl. 1, Fig. 4

Superfamily Primitiopoidea SWARTZ, 1936  
Family Primitiopsidae SWARTZ, 1936  
*Kielciella cf. fastigans* (BECKER, 1964)  
Pl. 1, Fig. 5

*Parapribylites hanaicus* POKORNY, 1950  
Pl. 1, Fig. 6

*Coryellina? audiarti* nov. sp.  
Pl. 1, Figs 8-10

*Urfetella adamczacki* BECKER, 1970  
Pl. 1, Fig. 11

Family Scrobiculidae POSNER, 1951  
*Roundyella patagiata* (BECKER, 1964)  
Pl. 1, Fig. 13

?Family Buregiidae POLENOVA, 1953  
*Buregia ovata* (KUMMEROW, 1953)  
Pl. 1, Fig. 15

Super-family unknown  
Family Kirkbyellidae SOHN, 1961  
*Refrathella struvei* BECKER, 1967  
Pl. 1, Fig. 12

Suborder Paraparchiticopina GRAMM in GRAMM & IVANOV (1975)

Superfamily Paraparchitoidea SCOTT, 1959  
Family Paraparchitidae SCOTT, 1959  
*Coeloenellina minima* (KUMMEROW, 1953)  
Pl. 1, Fig. 16

*Coeloenellina* n. sp. A, aff. *minima* (KUMMEROW, 1953)  
sensu CASIER & PRÉAT (1991)  
Pl. 1, Fig. 17

*Coeloenellina?* sp. indet.  
Pl. 1, Fig. 18

*Samarella* cf. *laevinodosa* BECKER, 1964  
Pl. 1, Fig. 14

Suborder Platycopina SARS, 1866  
Superfamily Kloedenelloidea ULRICH & BASSLER, 1908  
Family Kloedenellidae ULRICH & BASSLER, 1908  
*Poloniella tertia* KRÖMMELBEIN, 1953  
Pl. 2, Fig. 1

*Poloniella* cf. *claviformis* (KUMMEROW, 1953)  
Pl. 2, Fig. 2

*Uchtovia kloedenellides* (ADAMCZAK, 1968)  
Pl. 2, Fig. 7

*Uchtovia abundans* (POKORNY, 1950).  
Pl. 2, Figs 8-9

Family Beyrichiopsidae HENNINGSMOEN, 1953  
*Marginia* cf. *sculpta multicostata* POLENOVA, 1953  
Pl. 2, Fig. 3

Superfamily Cytherelloidea SARS, 1866  
Family Cavellinidae EGOROV, 1950  
*Cavellina macella* (KUMMEROW, 1953)?  
Pl. 2, Fig. 4

*Cavellina haursensis* nov. sp.  
Pl. 2, Figs 5-6

- ORDER PODOCOPIDA SARS, 1866  
 Suborder Metacopina SYLVESTER-BRADLEY, 1961  
 Superfamily Thlipsuroidea ULRICH, 1894  
   Family Thlipsuridae ULRICH, 1894  
     *Svantovites primus* POKORNY, 1950  
       Pl. 2, Figs 10-11
- Jefina romei* COEN, 1985?  
   Pl. 2, Fig. 12
- Family Bufinidae SOHN & STOVER, 1961  
   *Bufina schaderthalensis* ZAGORA, 1968  
     Pl. 2, Fig. 13
- Family Ropolonellidae CORYELL & MALKIN, 1936  
   *Ropolonellus ketneri* (POKORNY, 1950)  
     Pl. 2, Fig. 14
- Superfamily Healdoidea HARLTON, 1933  
   Family Healdiidae HARLTON, 1933  
     *Cytherellina obliqua* (KUMMEROW, 1953)  
       Pl. 2, Fig. 15
- Cytherellina perlonga* (KUMMEROW, 1953)  
   Pl. 2, Fig. 17
- Cytherellina?* cf. *brassicalis* BECKER, 1965  
   Pl. 2, Fig. 16
- Cytherellina* sp. A  
   Pl. 3, Fig. 1
- Cytherellina?* sp. indet.  
   Pl. 3, Fig. 2
- Suborder Podocopina SARS, 1866  
 Superfamily Bairdiocypridoidea SHAVER, 1961  
   Family Bairdiocyprididae SHAVER, 1961  
     *Healdianella* sp. A, aff. *budensis* OLEMPSKA, 1979  
       Pl. 3, Fig. 3
- Bairdiocypris rauffi* KRÖMMLBEIN, 1952  
   Pl. 3, Fig. 4
- Bairdiocypris* cf. *symmetrica* (KUMMEROW, 1953)  
   Pl. 3, Fig. 5
- Bairdiocypris* sp. A, aff. *eifliensis* (KEGEL, 1928)  
   Pl. 3, Fig. 6
- Baschkirina* sp. B in CASIER et al. (1992)?  
   Pl. 3, Fig. 7
- Family Bairdiocyprididae SHAVER, 1961?  
 "Orthocypris" sp. in CASIER et al. (1995)  
   Pl. 3, Fig. 8
- Family Pachydomellidae BERDAN & SOHN, 1961  
   *Microcheilinella affinis* POLENOVA, 1955  
     Pl. 3, Fig. 9
- Tubulibairdia clava* (KEGEL, 1933)  
   Pl. 3, Fig. 10
- Superfamily Bairdioidea SARS, 1888  
   Family Acratiidae GRÜNDEL, 1962  
     *Acratia* sp. A, aff. *Cechelovites cultratus* POKORNY, 1950  
       Pl. 3, Fig. 11
- Family Bairdiidae SARS, 1888  
   *Bairdia paffrathensis* KUMMEROW, 1953  
     Pl. 3, Fig. 12
- Bairdia* cf. *tischendorfi* BECKER, 1965  
   Pl. 3, Fig. 14
- Bairdia* cf. *carinata* POLENOVA, 1960, *sensu* COEN (1985)  
   Pl. 3, Fig. 13
- Bairdia* sp. A  
   Pl. 3, Fig. 15
- Bairdia* sp. B  
   Pl. 3, Fig. 16
- Bairdiacypris antiqua* (POKORNY, 1950)  
   Pl. 3, Fig. 17
- ORDER ERIDOSTRACA ADAMCZAK, 1961  
 Family Cryptophyllidae ADAMCZAK, 1961  
   *Cryptophyllus* sp. indet.  
     Pl. 3, Fig. 18
- Description of three new species*
- Parabolbinella coeni* nov. sp.  
   Fig. 4 in text; Pl. 1, Fig. 2
- ? p 1969 — *Falsipollex* sp. - GROOS, Pl. 18, Figs 11, 12.  
 v 1985 — *Falsipollex*? sp. - COEN, p. 9, Pl. 1, Fig. 5.  
 v 1988 — *Falsipollex*? sp 3G - MILHAU, p. 486, Pl. 55, Fig. 10.  
 v 1990 — *Parabolbinella*? sp. - CASIER & PRÉAT, p. 83, 84, Pl. 1, Fig. 8.  
 v 1991 — *Falsipollex*? sp 3G MILHAU, 1988 - CASIER & PRÉAT, Pl. 1, Fig. 8.  
 v 1992 — *Falsipollex* sp 3G MILHAU, 1988 - CASIER et al., Pl. 1, Fig. 8.  
 v 1993 — *Falsipollex* sp 3G MILHAU, 1988 - KASIMI, table 13-15, Pl. 16, Figs. 14, 15.  
 v 1995 — *Falsipollex*? sp 3G MILHAU, 1988 - CASIER et al., Pl. 64, Fig. 6  
 v 2010 — *Parabolbinella* nov. sp. A (= *Falsipollex*? sp. 3G in MILHAU (1988)) - CASIER et al., Pl. 4, Fig. 4.

2010 — *Parabolbinella cf. postaculeata* ADAMCZAK, 1968 - MAILLET, Pl. 3, Figs; 16, 17.

#### *Derivatio nominis*

The species is dedicated to Michel Coen who studied ostracods from the Mont d'Haur.

#### *Types*

Holotype: Left valve of a heteromorph (Fig. 4B *in text* = pl. 1, fig. 5 *in COEN, 1985*), left bank of the Houille River at Fromelennes, Fromelennes Fm, IRSNB n° b5455, L = 0.91; H = 0.46 mm. Paratype A: Left valve of a tecnomorph (Fig 4A *in text* = pl. 1, fig. 8 *in CASIER et al., 1992*), La Couvinoise Quarry, Ha 13, Hanonet Fm, IRSNB n° b 2477, L = 0.89 mm; H = 0.47 mm. Paratype B: Carapace of a juvenile (Fig 4C, 4D *in text* = pl. 64, fig. 6 *in CASIER et al., 1995*), Glageon Quarry, Trois-Fontaines Fm, IRSNB n° b 2691, L = 0.69 mm; H = 0.39; W = 0.33 mm.

#### *Material*

Twenty valves and one carapace from La Couvinoise and Resteigne quarries (Belgium), Mont d'Haur (Ardennes, France) and Glageon Quarry (Avesnois, France).

#### *Diagnosis*

*Parabolbinella* ADAMCZAK, 1968 with a well-rounded large L3 and an elliptic L2 perpendicular to the dorsal border. Posterior cardinal angle possibly with a

spine. Heteromorph with a long narrow frill. Surface papillose.

#### *Description*

Relatively large preplete bilobed Hollinidae SWARTZ, 1936, with a straight dorsal border. Anterior cardinal angle ranging from 105° up to 125°. Posterior cardinal angle ranging from 90° to 105° occasionally with a spine directed upwards. It might occur only on the left valve. Anterior margin more rounded than the posterior margin. Ventral border regularly curved. Great length between half and 1/3 of the great height toward the dorsal margin. The latter is located at 2/5 of the length. Well rounded large posterior lobe (L3) reaching the dorsal border in lateral view. Anterior lobe (L2) slightly elliptic with the major axis perpendicular to great length and located well below the dorsal border in lateral view. Anterior and posterior lobes joint by a ventral lobe delimiting a relatively deep adductor sulcus. A great width of the carapace corresponds to the anterior lobes. Tecnomorphs with two adventral spurs on each valve, the first one in the antero-ventral sector close to the 1/6 of the length, the second one in the postero-ventral sector, close the 3/5 of the length. Heteromorph larger with a narrow frill extending from the anterior cardinal angle to the 1/4 posterior of the carapace. The ornamentation is finely papillose but rarely preserved.

#### *Remarks*

The presence of a spine close to the posterior cardinal

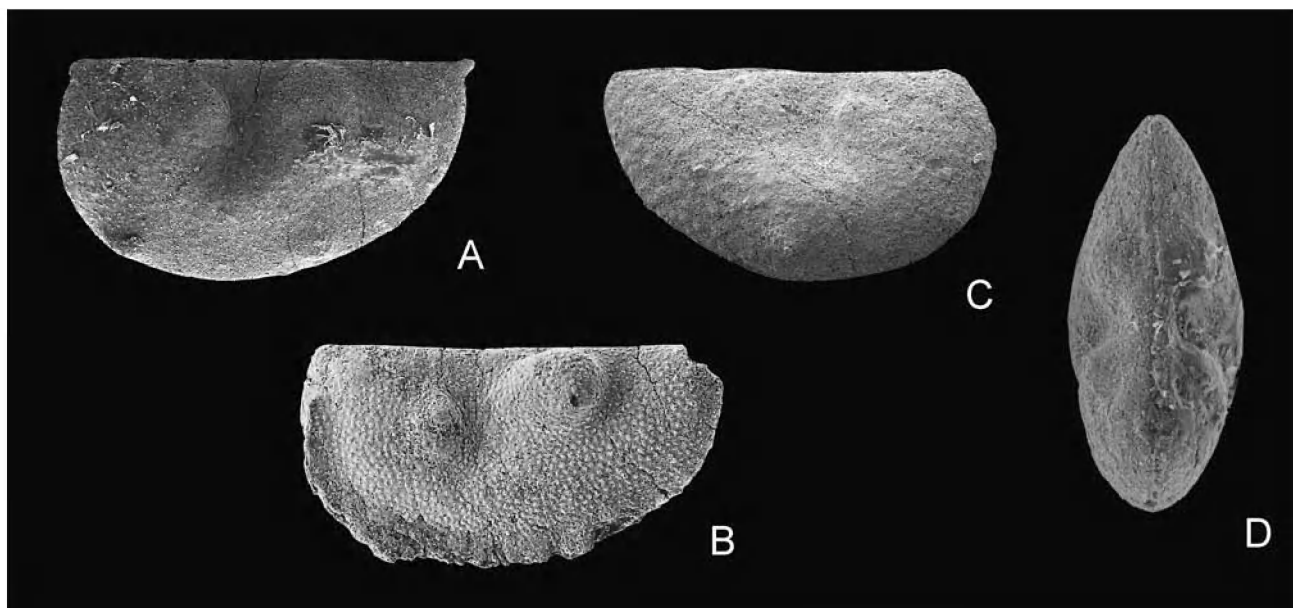


Fig. 4 — *Parabolbinella coeni* nov. sp. A. Paratype A, x80; B. Holotype, x80; C, D. Paratype B in a right lateral and dorsal view, x100.

angle is maybe linked to the low-energy environment. Several species belonging e.g. to the Thlipsuridae ULRICH, 1894, (e.g., in the genera *Favulella*, *Polyzygia*, *Svantovites*...) posses spiny subspecies (or ecotypes) in calm deep settings (CASIER, et al., 2010). But the absence of the spine on many carapaces of *Parabolbinella coeni* nov. sp. is maybe due to the poor preservation.

*Parabolbinella coeni* nov. sp. has been frequently assigned to the genus *Falsipollex* KESLING & MC MILLAN, 1951, but, firstly, in that genus the adventral spurs of tecnomorphs and the frills of heteromorphs are considerably more developed, secondly, the anterior (L2) and posterior (L3) lobes extend largely above the dorsal border in lateral view. The species is close to *Parabolbinella sufflatus* (BECKER, 1964) from the Middle Devonian in Eifel (Germany) but in that larger species, the ventral lobe is more developed. *Parabolbinella coeni* nov. sp. is also close to *Parabolbinella anteaculeata* ADAMCZAK, 1968, and to *Parabolbinella postaculeata* ADAMCZAK, 1968 from the Middle Devonian in the Holy Cross Mountains (Poland) but in these two species the frill is larger and never exceeds the mid-length.

Some specimens from the Givetian of the Bergischen Land and Sauerland (Germany) assigned to the genus *Falsipollex* by GROOS (1969, Pl. 18, Fig. 11, 12, not Fig. 20, 21) might be referred to *P. coeni* nov. sp.

The holotype formerly assigned with doubt to the genus *Falsipollex* by COEN (1985) has been collected from the base of the Fromelennes Fm outcropping on the left bank of the Houilles River at Fromelennes. The specimens figured by MAILLET (2010) have been collected in the same formation in the Flohimont section also at Fromelennes. *Falsipollex?* sp 3G of MILHAU (1988) was extracted from the Blacourt Fm in the Griset Quarry (Boulonnais, France). The *Parabolbinella?* sp. and the *Falsipollex?* sp 3G figured by CASIER & PRÉAT (1990, 1991), came from the Resteigne Quarry (Belgium). CASIER et al (1992, 1995) mentioned also the presence of *P. coeni* nov. sp. in the La Couvinoise Quarry (Belgium) and in the Glageon Quarry (Avesnois, France). Finally, KASIMI (1993) recognized the species in the Wellin Quarry and in the On-Jemelle Quarry (Belgium). In the Mont d'Haurs the new species is known from the upper part of the Hanonet Fm (Early Givetian) to the Mont d'Haurs Fm (study in progress).

#### Occurrence

Late Eifelian (Hanonet Fm) to Givetian (Hanonet Fm to Fromelennes Fm); Dinant Synclinorium (France and Belgium). Givetian of the Boulonnais (France).

#### *Coryellina? audiarti* nov. sp.

Pl. 1, Figs 8-10

- ? 1964 — *Coryellina* sp. G - MAGNE, Pl. 16, Fig. 30a, b.
- v 1974 — *Coryellina* sp. G. MAGNE, 1964 - BECKER & BLESS, Pl. 7, Fig. 4a, b.
- v 1990 — *Fellerites* sp. A - CASIER & PRÉAT, p. 85, Pl. 1, Fig. 15, 16.
- v 1991 — *Coryellina?* sp. A - CASIER & PRÉAT, Pl. 1, Fig. 21.
- v 1995 — *Fellerites* sp. - CASIER et al., Pl. 64, Fig. 10.

#### *Derivatio nominis*

The species is dedicated to Jacques Audiart who participated in our work at the Mont d'Haurs.

#### Types

Holotype: Carapace (Pl. 1, Figs 8a, b), MH-503, Hanonet Fm, IRSNB n° b5404, L = 0.62 mm; H = 0.40 mm; W = 0.31 mm. Paratype A: Carapace (Pl. 1, Fig. 9), MH-501, Hanonet Fm, IRSNB n° b5405, L = 0.57; H = 0.37; W = 0.30. Paratype B: Carapace (Pl. 1, Fig. 10), MH-501, Hanonet Fm, IRSNB n° b5406, L = 0.67; H = 0.43; W = 0.30.

#### Material

Eighteen carapaces and several valves. Six carapaces from the studied section, the others from Glageon (Avesnois, France) and Resteigne (Belgium).

#### Diagnosis

Middle-sized ostracod characterized by an angular dorsal border, by a straight hinge line in a long and narrow depression, and by a thin ridge along the free margin of both valves. No sulcus and no spines.

#### Description

Medium-sized amplete ostracod. Dorsal border angular with the summit of the 170° angle close to mid-length. Curvature of the anterior margin more accentuate dorsally with the anterior extremity at the 2/5 of the great height toward the dorsal margin. Posterior border more regularly rounded with the posterior extremity at mid-height. Ventral border slightly more curved in the anterior sector. Great length is achieved between half and 2/5 of the great height toward the dorsal margin. This one is located at mid-length. Left valve slightly larger than the right one and projecting along the free border, and occasionally along the dorsal border. Elliptic in dorsal view and straight hinge line in a long narrow depression. Thin ridge along the free margin of both valves. Great width at mid-length. Carapace smooth. Sexual dimorphism marked by a slight posterior thickening of the carapaces.

### Remarks

The *Coryellina* sp. G. MAGNE, 1964 figured by BECKER & BLESS (1974) has been collected from the Terres d'Haur Fm, at the Mont d'Haur. The specimens assigned to *Fellerites* sp. A and to *Coryellina?* sp. A by CASIER & PRÉAT (1990, 1991) come from the Hanonet Fm and from the Mont d'Haur Fm in the Resteigne Quarry, Belgium. The *Fellerites* sp. referred by CASIER et al. (1995) was extracted from the Trois-Fontaines Fm at Glageon, in the Avesnois, France.

*Coryellina curta* (POLENOVA in ROZHDESTVENSKAJA, 1959) from Baschkiria (Russian Federation) and the specimens from the Terres d'Haur Fm and from the Mont d'Haur Fm at the Mont d'Haur, assigned to this species by COEN (1985) posses more inflated valves, a broader dorsal depression, occasionally round tubercles close to the posterior extremity, and a more pronounced dimorphism. In fact, all these features (and occasionally the presence of a posterior spine on each valve) can be seen in most of species assigned to the genus *Coryellina* BRADFIELD, 1935.

The *Coryellina cybaea* (ROZHDESTVENSKAJA, 1959) identified by COEN (1985) in a sample collected in the base of the Fromelennes Fm at Philippeville posseses a medio-dorsal sinus, and a spine in the postero-ventral sector of the carapace.

The *Coryellina* sp. G figured by MAGNE (1964) is too poorly preserved to be unambiguously assigned to *Coryellina?* audiarti nov. sp.

### Occurrence

Givetian (Hanonet Fm to Mont d'Haur Fm); Dinant Synclinorium (France and Belgium).

### *Cavellina haursensis* nov. sp.

Pl. 2, Figs 5-6

v. 2010 — *Cavellina* sp. indet. - CASIER et al., Table 1, Pl. 5, Fig. 11.

### Derivatio nominis

From Mont d'Haur, the type section of the new species.

### Types

Holotype: Carapace (Pl. 2, Figs 5a, b), MH-523, Hanonet Fm, IRSNB n° b5419, L = 0.84 mm; H = 0.49 mm; W = 0.43 mm. Paratype A: Carapace (Pl. 2, Fig. 6), MH-527, Hanonet Fm, IRSNB n° b5420, L = 0.93; H = 0.42; W = 0.33. Paratype B: Carapace, MH-527, Hanonet Fm, IRSNB n° b5421, L = 0.66; H = 0.41; W = 0.35.

### Material

Five carapaces and two valves in the studied section, and one carapace in the Trois-Fontaines Fm exposed in the Rancennes Quarry at the Mont d'Haur.

### Diagnosis

Postplete pentagonal *Cavellina* CORYELL, 1928, with an angulose dorsal border. In left lateral view, right valve projecting slightly along the whole free margin and dorsal border.

### Description

Relatively large postplete pentagonal *Cavellina* CORYELL, 1928. Dorsal border more or less angular with the summit of the 150° angle close the 2/5 of the great length toward the posterior margin. Ventral margin quasi straight. Anterior part of the dorsal border almost straight. Anterior margin more rounded ventrally, and forming an angle with the dorsal border at the 1/10 of length and 1/3 of the height. Anterior extremity at the 1/4 of the great height toward the ventral margin. Posterior part of the dorsal border slightly curved and in continuity with more curved posterior border. Posterior extremity slightly below mid-height. Great length at the ventral 1/3 of the great height toward the ventral margin, and great hight at the 2/5 of the great length toward posterior margin. Right valve larger than left valve and projecting slightly along whole free margin and the dorsal border. Slight thickening of valves along the anterior and posterior margins. Biconvex in a dorsal view with the great width slightly posterior to the mid-length. Anterior extremity more rounded than the posterior one. Carapace smooth.

### Remarks

*Cavellina haursensis* nov. sp. is closely related to *Cavellina wahlensis* COEN, 1985 and to *Cavellina macella* KUMMEROW, 1953 occurring also at the Mont d'Haur. In these two species, the great high of the carapace is located close to the mid-length and there is no discontinuity between the dorsal border and the anterior border. Consequently these latter two species are more symmetric in lateral view than *Cavellina haursensis*.

### Occurrence

Givetian (Hanonet Fm and Trois-Fontaines Fm); Dinant Synclinorium (France).

### **Distribution of ostracods (Table 1)**

Ostracods are not abundant in the studied section and the diversity is variable. Forty-eight species were identified. Abundance varies mostly from one to ten specimens per 10 g sorted after the acetolysis. In five samples collected in the Hanonet Fm, the abundance varies from ten to twenty specimens per sample (MH-501, 502, 503, 505 and 507). In total, six samples from twenty-six (mostly from the top of the Hanonet Fm), were barren (MH-533, 536, 537, 538, 541, 607). A monospecific assemblage occurs in the sample MH-612 from the Trois-Fontaines Fm.

### **Paleoecology of ostracods**

The ostracods collected in the section belong to the Eifelian Mega-Assemblage indicative of shallow marine, semi-restricted or lagoonal environments. The first sample collected at the basal parts of the Hanonet Fm exposed in the studied section (sample MH-499) is poorly diversified and dominated by the large thick-shelled genus *Tubulibairdia* SWARTZ, 1936. This assemblage is indicative of an agitated environment close to the fair-weather wave base. Above, the fauna is more diversified up to the sample MH-507. For example, 23 species were identified in the sample MH-503. In this sample, the Platycopina, the Palaeocopina and the Metacopina are represented each by 5 species, and the Podocopina by 8 species. The large thick shelled genera *Tubulibairdia* SWARTZ, 1936, and *Bairdiocypris* KEGEL, 1932, also occur. This assemblage is indicative of a calm and well-oxygenated marine environment below fair-weather wave base. Abundance and diversity of ostracods decrease in the interval straddling the boundary between the Hanonet Fm and the Trois-Fontaines Fm and the Podocopina dominate. For instance, half the ostracod species belongs to the Podocopina in the samples MH-507 and MH-523. This is newly indicative of well-oxygenated relatively shallow-water conditions closer to fair-weather wave base. Ostracods are absent or broken and thus indeterminable in the following samples MH-531 to sample MH-541. The higher energy of the environment is probably responsible for poor preservation of these ostracods. The samples MH-543 and MH-608 collected in the Trois-Fontaines Fm are very rich in fragments of ostracods, which also point to the increased energy of the environment. Occurrence of Leperditicopid ostracods in thin section from the sample MH-611 is indicative of lagoonal conditions. Finally, the last sample (MH-612) includes numerous

specimens of *Coeloenellina* POLENOVA, 1952. The monospecific sample is indicative of a semi-restricted environments. These restricted water and even true lagoonal conditions characterized the middle and upper parts of the Trois-Fontaines Fm in the Rancennes Quarry (CASIER *et al.*, 2010).

### **Comparisons with ostracods previously identified at the Mont d'Haur and other sections**

On a poster presented during the 1<sup>st</sup> International Paleobiogeography Symposium held in Paris, MILHAU in HUBERT *et al.* (2007) reported 25 ostracod species in the Hanonet Fm and Trois-Fontaines Fm: *Bufina schaderthalensis* ZAGORA, 1968, *Ropolonellus kettneri* (POKORNY, 1950), *Poloniella tertia* KRÖMMELBEIN, 1953, *Urfella adamczaki* BECKER, 1970, *Quasillites fromelennensis* KUMMEROW, 1953, *Cytherellina obliqua* (KUMMEROW, 1953), *Uchtovia refrathensis* (KRÖMMELBEIN, 1954), *Bairdiocypris symmetrica* (KUMMEROW, 1953), *Amphicostella sculpturata* (POKORNY, 1950), *Bairdia paffrathensis* KUMMEROW, 1953, *Buregia ovata* (KUMMEROW, 1953), *Tubulibairdia seminalis* (KUMMEROW, 1953), *Uchtovia abundans* (POKORNY, 1950), *Refrathella struvei* BECKER, 1967, *Microcheilinella affinis* POLENOVA, 1955, *Amphissites tener omphalotus* BECKER, 1964, *Zeuschnerina dispar* ADAMCZAK, 1976, *Cytherellina groosae* COEN, 1985, *Samarella leavinodosa* BECKER, 1964, *Tubulibairdia clava* (KEGEL, 1933), *Bairdiocypris rauffi* KRÖMMELBEIN, 1952, *Uchtovia kloedenellides* (ADAMCZAK, 1968), *Svantovites primus* POKORNY, 1950, *Roundyella patagiata* BECKER, 1964, *Jenningsina heddebauti* MILHAU, 1983.

In this paper 18 of 25 species reported by MILHAU in HUBERT *et al.* (2007) were identified but it should be considered that *Samarella* cf. *laevinodosa* and *Bairdiocypris* cf. *symmetrica* reported herein correspond to *Samarella laevinodosa* and *Bairdiocypris symmetrica* of MILHAU (*ibid.*).

We did not find either *Amphicostella sculpturata* or *Zeuschnerina dispar* but these two species are generally rare. We also reported some specimens, which might belong to *Uchtovia refrathensis* MILHAU (*ibid.*) or to *Uchtovia abundans*, and others, which can be attributed to *Cytherellina groosae* or *Cytherellina obliqua*, the differences between these species being delicate.

*Quasillites fromelennensis* is absent in our samples but the majority of specimens collected by MILHAU (*ibid.*) came from an adjacent section probably deposited in a deeper setting. The occurrence of this species is

Table 1 – Distribution of ostracods in the Hanonet Fm and Trois-Fontaines Fm at the Mont d’Haurs.

MONT D'HAURS	499	500	501	502	503	505	507	508	511	516	521	523	525	527	543	604	608	610	612
<i>Poloniella tertia</i> KRÖMMLBEIN, 1953	●			●	●														
<i>Coryellina? audiarti</i> nov. sp.	●	●	●		●														
<i>Ropolonellus kettneri</i> (POKORNY, 1950)	●		●		●			●											
<i>Tubulibairdia clava</i> (KEGEL, 1933)	●	●	●	●	●	●	●	●	●	●	●	●	●	●					
<i>Uchtovia abundans</i> (POKORNY, 1950)	?	●		●	●		●				?	●	●	●					
<i>Bairdiocypris rauffi</i> KRÖMMLBEIN, 1952	●	●	●	●	●	●	●	?			●	●	●	●	?	?	?	?	
<i>Bufina schaderthalensis</i> ZAGORA, 1968		●	●	●	●	●	●												
<i>Cytherellina perlonga</i> (KUMMEROW, 1953)		●	●	●	●	●	●					●	●	●					
<i>Bairdia paffrathensis</i> KUMMEROW, 1953		●	●	●	●	●	●	●				●		?		?		?	
<i>Réfrathella struvei</i> BECKER, 1967			●			●													
<i>Jefina romei</i> COEN, 1985?			●			●													
<i>Parabolbinella coeni</i> nov. sp.			●				●												
“ <i>Orthocypris</i> ” sp. in CASIER et al. (1995)			●		●	●	●												
<i>Bairdiocypris cf. symmetrica</i> (KUMMEROW, 1953)			●		●						●								
<i>Amphissites tener omphalotus</i> BECKER, 1964			●		●		●				?								
<i>Bairdia cf. carinata</i> POLENOVA, 1960 <i>sensu</i> COEN (1985)			●		●							●							
<i>Samarella cf. laevinodosa</i> BECKER, 1964			●					?			●	●	●						
<i>Cavellina haursensis</i> nov. sp.			●		●						●	●	●						
<i>Urfella adamczacki</i> BECKER, 1970			●						●					●					
<i>Cytherellina? cf. brassicalis</i> BECKER, 1965			●	●	●	●	●	?						●	?				
<i>Cytherellina obliqua</i> (KUMMEROW, 1953)			●	●	●	●	●	?						●	●				
<i>Poloniella cf. claviformis</i> (KUMMEROW, 1953)				●															
<i>Acratia</i> sp. A				●															
<i>Uchtovia kloedenellides</i> (ADAMCZAK, 1968)				●	●		●		●				?	?	?	?	?		
<i>Kozlowskiella</i> sp. C in CASIER et al. (1994)				?	?		?							●					
<i>Cryptophyllus</i> sp. indet.				●													●		
<i>Marginia</i> cf. <i>sculpta multicostata</i> POLENOVA, 1953					●														
<i>Bairdia</i> sp. A						●													
<i>Roundyella patagiata</i> (BECKER, 1964)						●	●												
<i>Bairdia cf. tischendorfi</i> BECKER, 1965						●	●	●	?	?									
<i>Parapribylites hanaicus</i> POKORNY, 1950						●							?					●	
<i>Microcheilinella affinis</i> POLENOVA, 1955							●					●	●		?	●	?	●	
<i>Svantovites primus</i> POKORNY, 1950								●											
<i>Cytherellina?</i> sp. indet.								●											
<i>Bairdiocypris</i> sp. A, aff. <i>eifliensis</i> (KEGEL, 1928)							●												
<i>Healdianella</i> sp. A, aff. <i>budensis</i> OLEMPSKA, 1979								●	?			?	●	●			●		
<i>Cytherellina</i> sp. A										●									
<i>Baschkirina</i> sp. B in CASIER et al. (1992)?														●					
<i>Coeloenellina</i> sp. A, aff. <i>minima</i> (KUMMEROW, 1953)												●	●	●				●	
<i>Buregia ovata</i> (KUMMEROW, 1953)													●						
<i>Bairdia</i> sp. B													●						
<i>Aparchites</i> sp. A in CASIER et al. (2010)													●	●					
<i>Fellerites crumena</i> (KUMMEROW, 1953)														●					
<i>Coeloenellina?</i> sp. indet.														●					
<i>Coeloenellina minima</i> (KUMMEROW, 1953)														●				●	
<i>Kielciella</i> cf. <i>fastigans</i> (BECKER, 1964)														●					
<i>Cavellina macella</i> (KUMMEROW, 1953)															?				
<i>Bairdiacypris antiqua</i> POKORNY, 1950																●			

important because this one would characterize a new zone of the zonal sequence established on metacopids in the Devonian by CASIER (1979; 2008).

Most of species identified in the Rancennes Quarry are known from other sections in the Dinant Synclinorium, particularly from the Resteigne Quarry (CASIER & PRÉAT, 1990, 1991) and La Couvinoise Quarry (CASIER *et al.*, 1992), in Belgium and also from the Glageon Quarry, in Avesnois (CASIER *et al.*, 1995), France. Close relationship exists also among ostracods from the Aisemont Quarry in the Namur Synclinorium (CASIER & PRÉAT, 2006), Boulonnais in France (MAGNE, 1964; MILHAU, 1988), Eifel in Germany (KUMMEROW, 1953; BECKER, 1964, 1965; GROOS, 1969...), Holy Cross Mountains in Poland (ADAMCZAK, 1968, 1976; OLEMPSKA 1979; ZBIKOWSKA, 1983...), and the Czech Republic (POKORNY, 1950).

## Conclusions

The ostracod fauna collected in the upper part of the Hanonet Fm and in the base of the Trois-Fontaines Fm at the Mont d’Haurs, belongs to the Eifelian Mega-Assemblage and is indicative of shallow marine well-oxygenated environments generally close to fair-weather wave base. Only one sample collected at the top of the section studied contains an ostracod assemblage indicative of semi-restricted water conditions (in this sample the monospecific assemblage with the genus *Coeleonellina* prevails), and another sample from the same part of the section, contains Leperditicopid ostracods indicative of lagoonal environmental conditions. Three new species are described: *Coryellina?* *audiarti* nov. sp., *Cavellina haursensis* nov. sp and *Parabolbinella coeni* nov. sp.

$X_{LF}$  values decrease across the boundary interval between the Hanonet Fm and the Trois-Fontaines Fm and are very weak during the biostromal unit, before reaching the highest  $X_{LF}$  values in the restricted lagoonal environment of the Trois-Fontaines Fm.  $X_{LF}$  and microfacies curves show a moderate positive correlation in general. This is due to the evolution from a mixed ramp (Hanonet Fm) to a carbonate platform (Trois-Fontaines Fm).

A high-resolution stratigraphic correlation is tentatively proposed here between the Mont d’Haurs section and a 40 km-distant Baileux section where similar MS fluctuations were reported (MABILLE & BOULVAIN, 2008) even if the sediments in the Baileux section are much thicker. The MS signal is strongly controlled by ferromagnetic *s.l.* minerals (mixture of magnetite with

significant contribution of a high-coercivity phase, which might be hematite) and paramagnetic grains. The transition from a mixed- to inner-ramp system to a restricted lagoon in the carbonate platform system is accompanied by sea-level fall and an input of coarse-grained ferromagnetic *s.l.* minerals (probably of detrital origin). However, an increasing trend of the  $S_d$  and IRM loss parameters is observed across the section with the highest values (together with the  $X_{LF}$  values) in the lagoonal sediments of the Trois-Fontaines Fm. These two parameters point to the occurrence of a significant proportion of ultrafine-grained magnetite (close to 30 nm) probably formed during diagenesis. The primary MS signal is thus affected by diagenetic processes, which slightly modified the magnetic signal of the lagoonal limestones after deposition.

## Acknowledgments

The research has been supported by the FRFC n° 2.4518.07 project of the Belgian “Fonds National de la Recherche Scientifique (FNRS) and contributes to the IGCP Project No.580 “Application of magnetic susceptibility on Paleozoic sedimentary rocks”. The hysteresis analyses were carried out at the Geophysical Centre of the Belgian Royal Meteorological Institute and Simo Spassov is greatly acknowledged for easy access to the laboratory. We thank especially Marie Coen-Aubert for providing of the specimen figured by Michel Coen in his paper on the Givetian ostracods, and designed herein as holotype for the new species *Parabolbinella coeni* nov. sp. She is also thanked for the storing of all figured specimens and types of her deceased husband into the collection of Department of Paleontology of the Royal Belgian Institute of natural Sciences. We appreciate the helpful review of our manuscript by Dr. L. Koptikova (Prague) and Dr. R. Gozalo (Valencia). Finally, we thanks Mr. Rigo who has kindly authorised the access to the section.

## References

- ADAMCZAK, F., 1968. Palaeocopa and Platycopa (Ostracoda) from Middle Devonian rocks in the Holy Cross Mountains, Poland. *Stockholm Contributions in Geology*, **57**, 109 pp.
- ADAMCZAK, F., 1976. Middle Devonian Podocopida (Ostracoda) from Poland; their morphology, systematics and occurrence. *Senckenbergiana Lethaea*, **57**, 4-6: 265-467.
- AHR, W.M., 1973. The carbonate ramp: an alternative to the shelf model. *Gulf Coast Association of Geologic Societies Transactions*, **23**: 221-225.
- AIGNER, T., 1985. Storm depositional systems. Dynamic stratigraphy on modern and ancient shallow-marine sequences. Lecture Notes in Earth Sciences, Springer Verlag, Berlin, Heidelberg, New-York, 174 pp.
- ANDREWS, J.T., & STRAVERS, J.A., 1993. Magnetic susceptibility of late Quaternary marine sediments, Frobisher

- Bay, N.W.T.: an indicator of changes in provenance and process. *Quaternary Science Reviews*, **12**: 157-168.
- ANTROPOV, I.A., 1959. Devonian Foraminifera of Tatatria. *Akademy Nauk SSSR Kazanskoye Filial, Izvestia Seriia Geologik*, **1**: 11-33 (in Russian).
- BECKER, G., 1964. Palaeocopida (Ostracoda) aus dem Mitteldevon der Sötenicher Mulde (N-Eifel). *Senckenbergiana Lethaea*, **45**, 1-4: 43-113.
- BECKER, G., 1965. Podocopida (Ostracoda) aus dem Mitteldevon der Sötenicher Mulde (N-Eifel). *Senckenbergiana Lethaea*, **46**, 4-6: 367-441.
- BECKER, G. & BLESS, M., 1974. Ostracode stratigraphy of the Ardenno-Rhenish Devonian and Dinantian. In: BOUCKAERT, J. & STREEL, M. (eds), Publication of the International Symposium on Belgian Micropaleontological limits, Namur, **1**, 52 pp.
- BIRINA, L.M., 1948. A detailed scheme of the stratigraphy of the passage beds between the Devonian and the Carboniferous (Etroeungt) in the southern part of the Podmoscovian region. *Sovjetskaia Geologia*, **28**: 146-153 (in Russian).
- BLOEMENDAL, J., KING, J.W., TAUXE, L. & VALET, J.-P., 1989. Rock magnetic stratigraphy of Leg 108 Sites 658, 659, 661 and 665, eastern tropical Atlantic. In: RUDDIMAN, W.F. et al. (eds), Proceedings of the Ocean Drilling Program, Initial Reports, **108** (College Station, TX): 415-428.
- BORRADAILE, G.J. & LAGROIX, F., 2000. Magnetic characterization using a three-dimensional hysteresis projection, illustrated with a study of limestones. *Geophysical Journal International*, **141**: 213-226.
- BULTYNCK, P., 1987. Pelagic and neritic conodont successions from the Givetian of pre-Saharan Morocco and the Ardennes. *Bulletin de l'Institut royal des Sciences naturelles de Belgique, Sciences de la Terre*, **57**: 149-181.
- BULTYNCK, P., COEN-AUBERT, M., DEJONGHE, L., GODEFROID, J., HANCE, L., LACROIX, D., PRÉAT, A., STAINIER, P., STEEMANS, P., STREEL, M. & TOURNEUR, F., 1991. Les formations du Dévonien Moyen de la Belgique. *Mémoires pour servir à l'explication des cartes géologiques et minières de la Belgique*, **30**, 105 pp.
- BULTYNCK, P. & DEJONGHE, L., 2001. Devonian lithostratigraphic units (Belgium). *Geologica Belgica*, **4** (1-2): 39-69.
- BULTYNCK, P. & HOLLEVOET, C., 1999. The Eifelian-Givetian boundary and Struve's Middle Devonian Great Gap in the Couvin area (Ardennes, southern Belgium). *Senckenbergiana Lethaea*, **789**: 3-11.
- BUROV, B., NURGALIEV, D.K. & JASONOV, P.G., 1986. Paleomagnetic Analysis. Kazan University Press: 176 pp. (in Russian).
- CASIER, J.-G., 1979. La Zone à *Svantovites lethiersi* n. sp., zone nouvelle d'Ostracodes de la fin du Frasnien et du début du Famennien. *Bulletin de l'Institut royal des Sciences naturelles de Belgique, Sciences de la Terre*, **51**, 15, 7 pp.
- CASIER, J.-G., 2008. Guide de l'excursion: Les ostracodes du Dévonien Moyen et Supérieur du Synclinorium de Dinant. In: J.-G. CASIER, Résumé des communications et guide de l'excursion 22<sup>ème</sup> Réunion des Ostracodologues de langue française, Bruxelles 2-4 juin. Institut royal des Sciences naturelles de Belgique, 83 pp.
- CASIER, J.-G. & PRÉAT, A., 1990. Sédimentologie et Ostracodes de la limite Eifelien-Givetien à Resteigne (bord sud du Bassin de Dinant, Belgique). *Bulletin de l'Institut royal des Sciences naturelles de Belgique, Sciences de la Terre*, **60**: 75-105.
- CASIER, J.-G. & PRÉAT, A., 1991. Evolution sédimentaire et Ostracodes de la base du Givetien à Resteigne (bord sud du Bassin de Dinant, Belgique). *Bulletin de l'Institut royal des Sciences naturelles de Belgique, Sciences de la Terre*, **61**: 155-177.
- CASIER, J.-G. & PRÉAT, A., 2006. Ostracodes and lithofacies close to the Eifelian-Givetian boundary (Devonian) at Aisemont (Namur Synclinorium, Belgium). *Bulletin de l'Institut royal des Sciences naturelles de Belgique, Sciences de la Terre*, **76**: 5-29.
- CASIER, J.-G., PRÉAT, A. & KASIMI, R., 1992. Ostracodes et sédimentologie du sommet de l'Eifelien et de la Base du Givetien, à Couvin (bord sud du Bassin de Dinant). *Bulletin de l'Institut royal des Sciences naturelles de Belgique, Sciences de la Terre*, **62**: 75-108.
- CASIER, J.-G., KASIMI, R. & PRÉAT, A., 1995. Les Ostracodes au passage Eifelien/Givetien à Glageon (Avesnois, France). *Géobios*, **28** (4): 487-499.
- CASIER, J.-G., LEBON, A., MAMET, B. & PRÉAT, A., 2005. Ostracodes and lithofacies close to the Devonian-Carboniferous boundary in the Chanxhe and Rivage sections, northeastern part of the Dinant Basin, Belgium. *Bulletin de l'Institut royal des Sciences naturelles de Belgique, Sciences de la Terre*, **75**: 95-126.
- CASIER, J.-G., CAMBIER, G., DEVLEESCHOUWER, X., PETITCLERC, E. & PRÉAT, A., 2010. Ostracods, rock facies and magnetic susceptibility of the Trois-Fontaines and Terres d'Haur Formation (Early Givetian) in the Rancennes Quarry at the Mont d'Haur (Givet, France). *Bulletin de l'Institut royal des Sciences naturelles de Belgique, Sciences de la Terre*, **80**: 85-114.
- CHEN, T., HUIFANG, X., XIE, Q., CHEN, J., JI, J. & LU, H., 2005. Characteristics and genesis of maghemite in Chinese loess and paleosols: mechanism for magnetic susceptibility enhancement in paleosols. *Earth and Planetary Science Letters*, **240**: 790-802.
- COEN, M., 1985. Ostracodes givétiens de l'Ardenne. *Mémoires de l'Institut géologique de l'Université de Louvain*, **32**, 48 pp.

- COEN-AUBERT, M., PRÉAT, A. & TOURNEUR, F., 1986. Compte-rendu de l'excursion de la Société belge de Géologie du 6 novembre 1985 consacrée à l'étude du sommet du Couvinien et du Givétien au bord sud du Bassin de Dinant, de Resteigne à Beauraing. *Bulletin de la Société belge de Géologie*, **95** (4): 247-256.
- CRICK, R.E., ELLWOOD, B. & EL HASSANI, A., 1994. Integration of biostratigraphy, magnetic susceptibility and relative sea-level change: a new look at high resolution correlation. *Subcommission on Devonian Stratigraphy Newsletter*, **11**: 59-66.
- CRICK, R.E., ELLWOOD, B., EL HASSANI, A. & FEIST, R., 2000. Proposed magnetostratigraphy susceptibility magnetostratotype for the Eifelian-Givetian GSSP (Anti-Atlas, Morocco). *Episodes*, **23** (2): 93-101.
- CRICK, R.E., ELLWOOD, B., EL HASSANI, A., FEIST, R. & HLADIL, J., 1997. MagnetoSusceptibility Event and Cyclostratigraphy (MSEC) of the Eifelian-Givetian GSSP and associate boundary sequences in north Africa and Europe. *Episodes*, **20** (3): 167-175.
- CRICK, R.E., ELLWOOD, B.B., HLADIL, J., EL HASSANI, A., HROUDA, F. & CHLUPAC, I., 2001. Magnetostratigraphy susceptibility of the Pridolian-Lochkovian (Silurian-Devonian) GSSP (Klonk, Czech Republic) and coeval sequence in Anti-Atlas Morocco. *Palaeogeography Palaeoclimatology Palaeoecology*, **167**: 73-100.
- DA SILVA, A.C., MABILLE, C. & BOULVAIN, F., 2009. Influence of sedimentary setting on the use of magnetic susceptibility: examples from the Devonian of Belgium. *Sedimentology*, **56**: 1292-1306.
- DEVLEESCHOUWER, X., 1999. La limite Frasnien-Famennien (Dévonien Supérieur) en Europe: sédimentologie, stratigraphie séquentielle et susceptibilité magnétique. Université Libre de Bruxelles et Université des Sciences et Technologies de Lille, 414 p. (Thèse de Doctorat en Sciences géologiques et minéralogiques, unpublished).
- DEVLEESCHOUWER, X., PETITCLERC, E., SPASSOV, S. & PRÉAT, A., 2010. The Givetian-Frasnian boundary at Nismes parastratotype (Belgium): the magnetic susceptibility signal controlled by ferromagnetic minerals. *Geologica Belgica*, **13** (4): 345-360.
- DEVLEESCHOUWER, X., PRÉAT, A., AVERBUCH, A. & HERBOSCH, A. 1999. Magnetic susceptibility through the Frasnian-Famennian boundary (Steinbruch Schmidt, Germany and Coumiac, France). *Abstract book 19th regional European Meeting of Sedimentology, Copenhagen, Denmark*: 71-72.
- DUNLOP, D.J., 2002. Theory and applications of the Day Plot (Mrs/Ms versus Hcr/Hc): 1. Theoretical curves and tests using titanomagnetite data. *Journal of Geophysical Research*, **107**, B3, doi: 10.1029/2001JB000486.
- EINSELE, G. & SEILACHER, A., (Eds), 1982. Cyclic and Event Stratification. Springer, Berlin, Heidelberg, New York, 536 pp.
- ELLWOOD, B., BENOIST, S.L., EL HASSANI, A., WHEELER, C. & CRICK, R.E., 2003. Impact ejecta layer from the Mid-Devonian: possible connection to global mass extinctions. *Science*, **300** (5626): 1734-1737.
- ELLWOOD, B., BRETT, C.E. & MACDONALD, W.D., 2007. Magnetostratigraphy susceptibility of the Upper Ordovician Kope Formation, northern Kentucky. *Palaeogeography Palaeoclimatology Palaeoecology*, **243**: 42-54.
- ELLWOOD, B., CRICK, R.E. & EL HASSANI, A., 1999. The Magneto-Susceptibility Event and Cyclostratigraphy (MSEC) method used in geological correlation of Devonian rocks from Anti-Atlas Morocco. *American Association of Petroleum Geology Bulletin*, **83** (7): 1119-1134.
- ELLWOOD, B., CRICK, R.E., EL HASSANI, A., BENOIST, S.L. & YOUNG, R.H., 2000. Magnetosusceptibility event and cyclostratigraphy method applied to marine rocks: detrital input versus carbonate productivity. *Geology*, **28** (12): 1135-1138.
- ELLWOOD, B., CRICK, R.E., GARCIA-ALCALDE FERNANDEZ, J.L., SOTO, F.M., TRUYOLS-MASSONI, M., EL HASSANI, A. & KOVAS, E.J., 2001. Global correlation using magnetic susceptibility data from Lower Devonian rocks. *Geology*, **29** (7): 583-586.
- ELLWOOD, B., TOMKIN, J.H., RATCLIFFE, K.T., WRIGHT, M. & KAFAFY, A.M., 2008. High-resolution magnetic susceptibility and geochemistry for the Cenomanian/Turonian boundary GSSP with correlation to time equivalent core. *Palaeogeography Palaeoclimatology Palaeoecology*, **261**: 105-126.
- ENOS, P., 1983. Shelf. In: SCHOLLE, P.A., BEBOUT, D.G., MOORE, C.H. (eds), Carbonate Depositional Environments. *Memoirs American Association of Petroleum Geologists*, **33**: 267-296.
- ERRERA, M., MAMET, B. & SARTENAER, P., 1972. Le calcaire de Givet et le Givétien à Givet. *Bulletin de l'Institut royal des Sciences naturelles de Belgique, Sciences de la Terre*, **48** (1): 59 pp.
- EVANS, M.E. & HELLER, F., 2003. Environmental magnetism. Principles and Applications of Enviromagnetics. Academic Press, Elsevier Science: 299 pp.
- GARWOOD, E.J., 1931. Important additions to our knowledge of the fossil calcareous algae since 1913 with special reference to the Precambrian and Paleozoic rocks. *Quaternary Journal of the Geological Society of London*, **87**: 48-100.
- GORBARENKO, S.A., NUERNBERG, D., DERKACHEV, A.N., ASTAKHOV, A.S., SOUTHON, J.R. & KAISER, A., 2002. Magnetostratigraphy and tephrochronology of the upper Quaternary sediments in the Okhotsk Sea: implication of terrigenous, volcanicogenic and biogenic matter supply. *Marine Geology*, **183**: 107-129.

- GROOS, H., 1969. Mitteldevonische Ostracoden zwischen Ruhr und Sieg (Rechtsrheinisches Schiefergebirge). *Göttinger Arbeiten zur Geologie und Paläontologie*, **1**, 110 pp.
- GUILLERIN, Y., 1979. Eléments de pétrographie des évaporites oligocènes des bassins de la Bresse et de Valence (Est de la France, Vallée de la Saône et du Rhône) = pp. 41-48 in: *Les dépôts évaporitiques, illustration et interprétation de quelques séquences*, Editions Technip, Paris.
- HLADIL, J., 2002. Geophysical records of dispersed weathering products on the Frasnian carbonate platform and early Famennian ramps in Moravia, Czech Republic: proxies for eustasy and paleoclimate. *Palaeogeography Palaeoclimatology Palaeoecology*, **181**: 213-250.
- HLADIL, J., CAREW, J.L., MYLROIE, J.E., PRUNER, P., KOHOUT, T., JELL, J.S., LACKA, B. & LANGROVA, A., 2004. Anomalous magnetic susceptibility values and traces of subsurface microbial activity in carbonate banks on San Salvador Island, Bahamas. *Facies*, **50**: 161-182.
- HLADIL, J., GERSL, M., STRNAD, L., FRANA, J., LANGROVA, A. & SPISIAK, J., 2006. Stratigraphic variation of complex impurities in platform limestones and possible significance of atmospheric dust: a study with emphasis on gamma-ray spectrometry and magnetic susceptibility outcrop logging (Eifelian-Frasnian, Moravia, Czech Republic). *International Journal of Earth Sciences*, **95**: 703-723.
- HORBURY, A.D. & ADAMS, A.E., 1996. Microfacies associations in Asbian carbonates: an example from the Uswick Limestone Formation of the southern Lake District, northern England. *Geological Society of London, Special Publication*, **107**: 221-237.
- HUBERT, B., 2008. Detailed lithology and faunal occurrence of the historical Givetian section: the fortifications of the Mont d'Haurs (Givet, France). *Annales de la Société géologique du Nord*, **15**, 2<sup>ème</sup> sér.: 53-65.
- HUBERT, B., BRICE, D., CRONIER, C., MILHAU, B., MISTIAEN, B., NICOLLIN, J.-P., & ZAPALSKI, M., 2007. Distribution of stromatoporoids, tabulate corals, brachiopods, trilobites and ostracods around the Hanonet - Trois-Fontaines formations boundary (Givet, France) - Affinities and paleogeographical implications. Abstract 1<sup>st</sup> International Palaeogeography Symposium, Paris 10-13 July: 49.
- KAHLE, F.C., 1977. Origin of subaerial Holocene calcareous crusts: role of algae, fungi and sparmicritisation. *Sedimentology*, **24**: 413-435.
- KASIMI, R., 1993. Sédimentologie et cyclostratigraphie des couches de transition Eifelian - Givetien au bord sud du Bassin de Dinant (Belgique, France). Unpublished Ph.D University of Brussels, 273 pp.
- KASIMI, R., & PRÉAT, A., 1996. Sédimentation de rampe mixte silico-carbonatée des couches de transition eifeliennes-givétiennes franco-belges. Deuxième partie: Cyclostratigraphie et paléostructure. *Bulletin des Centres de Recherches Exploration-Production Elf-Aquitaine*, **20** (1): 61-90.
- KUMMEROW, E., 1953. Über oberkarbonische und devonische Ostracoden in Deutschland und in der Volksrepublik Polen. *Geologie*, **7**, 75 pp.
- KRÖMMELBEIN, K., 1953. Ostrakoden-Studien im Devon der Eifel - 3: Nachweis der polnischen Gattungen *Polyzygia* und *Poloniella* im Mittel-Devon der Eifel. *Senckenbergiana*, **34** (1-3): 53-59.
- LANGER, W., 1979. Neue karbonatische Microproblematika aus dem westdeutschen Devon. *Neues Jahrbuch für Geologie und Paläontologie Monatshefte*, **12**: 723-733.
- LETHIERS, F. & CRASQUIN-SOLEAU, S., 1988. Comment extraire les microfossiles à tests calcitiques des roches calcaires dures. *Revue de Micropaléontologie*, **31** (1): 56-61.
- MABILLE, C. & BOULVAIN, F., 2007. Sedimentology and magnetic susceptibility of the Couvin Formation (Eifelian, south western Belgium): carbonate platform initiation in a hostile world. *Geologica Belgica*, **10** (1-2): 47-67.
- MABILLE, C. & BOULVAIN, F., 2008. Les Monts de Baileux section: detailed sedimentology and magnetic susceptibility of Hanonet, Trois-Fontaines and Terres d'Haurs Formations (Eifelian/Givetian boundary and Lower Givetian, SW Belgium). *Geologica Belgica*, **11**: 93-121.
- MAGNE, F., 1964. Données micropaléontologiques et stratigraphiques dans le Dévonien du Boulonnais (France) et du Bassin de Namur (Belgique). Thèse de 3<sup>ème</sup> cycle, Université de Paris, Société nationale des Pétroles d'Aquitaine, Centre de Recherches de Pau, 172 pp.
- MAILLET, S., 2010. Les ostracodes du Givétien supérieur au bord sud du Synclinorium de Dinant (Formation de Fromelles, région de Givet, Ardennes): biostratigraphie, paléocologie, recherche de bioévénements. Unpublished Master thesis in Environment, University of Lille 1, 40 pp.
- MAMET, B. & PRÉAT, A., 1985. Sur quelques Algues Vertes nouvelles du Givétien de la Belgique. *Revue de Micropaléontologie*, **28**: 67-74.
- MAMET, B. & PRÉAT, A., 2005. Microfaciès d'une lentille biohermale à la limite Eifélien-Givetien (Wellin, bord sud du Synclinorium de Dinant). *Geologica Belgica*, **8** (3): 85-111.
- MAMET, B. & PRÉAT, A., 2009. Algues et microfossiles problématiques du Dévonien Moyen du "Fondry des Chiens" (bord sud du Synclinorium de Dinant, Belgique): implications paléobathymétriques. *Revue de Micropaléontologie*, **52**: 249-263.
- MAMET, B. & ROUX, A., 1981. Note sur le genre *Issinella* (algue paléozoïque). *Revue de Micropaléontologie*, **23** (3-4): 151-158.
- MILHAU, B., 1988. Ostracodes du Givétien de Ferques

- (Dévonien Moyen, Boulonnais, France). In: D. BRICE (ed.), Le Dévonien de Ferques, Bas-Boulonnais (N. France). *Biostratigraphie du Paléozoïque*, 7: 479-491.
- OLEMPSKA, E., 1979. Middle to Upper Devonian Ostracoda from the Southern Holy Cross Mountains, Poland. *Palaeontologica Polonica*, 40: 57-162.
- POKORNY, V., 1950. Skorepatci strednodevonskych "cervenyh vapencu koralovych" z Celechovic. *Sbornik Statniho Geologickeho Ustavu Ceskoslovenske Republiky Oddil Paleontologicky*, 17: 513-632.
- PRÉAT, A. & MAMET, B., 1989. Sédimentation de la plate-forme carbonatée givétienne franco-belge. *Bulletin des Centres de Recherche Exploration-Production Elf-Aquitaine*, 13, (1): 47-86.
- PRÉAT, A., BLOCKMANS, S., CAPETTE, L., DUMOULIN, V. & MAMET, B., 2007. Microfaciès d'une lentille biohermale à la limite Eifélien-Givétien ("Fondry des Chiens", Nismes, bord sud du Synclinorium de Dinant). *Geologica Belgica*, 10 (1-2): 3-25.
- PRÉAT, A. & KASIMI, R., 1995. Sédimentation de rampe mixte silico-carbonatée des couches de transition eiféliennes-givétienes franco-belges. Première partie: microfaciès et modèle sédimentaire. *Bulletin des Centres de Recherche Exploration-Production Elf-Aquitaine*, 19 (2): 329-375.
- RIQUIER, L., AVERBUCH, O., DEVLEESCHOUWER, X. & TRIBOVILLARD, N., 2010. Rock magnetic evidences for a major climatic transition at the Frasnian-Famennian boundary (ca 375 Ma BP). *International Journal of Earth Sciences*, 99: S57-S73. DOI 10.1007/s00531-009-0492-7.
- ROBINSON, S.G., 1993. Lithostratigraphic applications for magnetic susceptibility logging of deep sea sediment cores: examples from ODP Leg 115. In: HAILWOOD, E.A., KIDD, R.B., (eds.). High Resolution Stratigraphy. *Geological Society of London, Special Publication*, 70: 65-98.
- ROZHDESTVENSKAJA, A., 1959. Ostrakody terrigennoy tolshchi Devona zapadnoy Bashkirii i ikh stratigraficheskoe znachenie. In: E. CHRIBIKOVA & A. ROZHDESTVENSKAJA (eds). Materialy po paleontologii i stratigrafiu Devonskikh i bolee drevnikh otlozheniy Bashkirii: 117-247.
- SHINN, E.A., 1968. Practical significance of birdseyes structures in carbonate rocks. *Journal of Sedimentary Petrology*, 38 (1): 215-223.
- SHINN, E.A., 1983. Birdseyes, fenestrae, shrinkage pores and loferites: a reevaluation. *Journal of Sedimentary Petrology*, 53: 619-628.
- TEBBUTT, G.E., CONLEY, C.D. & BOYD, D.W., 1965. Lithogenesis of a carbonate rock fabric. *Contribution in Geology*, 4 (1): 1-1.
- VAIL, P.R., AUDEMARD, F., BOWMAN, S.A., EISNER, P.N. & PEREZ-CRUZ, C., 1991. The stratigraphic signatures of tectonics, eustacy and sedimentology. An overview. In: EINSELE, G., RICKEN, W. & SEILACHER, A. (eds). *Cycles and events in stratigraphy*. Springer Verlag, Berlin: 617-659.
- VANDERAVEROET, P., AVERBUCH, O., DECONINCK, J.-F. & CHAMLEY, H., 1999. Glacial/interglacial cycles in Pleistocene sediments of New Jersey expressed by clay minerals, grain size and magnetic susceptibility data. *Marine Geology*, 159: 79-92.
- VAN WAGONER, J.C., MITCHUM, R.M., POSAMENTIER, H.W. & VAIL, P.R., 1987. Seismic stratigraphy interpretation using sequence stratigraphy. Part II: the key definitions of sequence stratigraphy. In: BALLY, A.W. (ed.), *Atlas of seismic stratigraphy 1. American Association of Petroleum Geologists, Studies in Geology*, 27: 11-14.
- WAGNER, C.W. & VAN DER TOGT, C., 1973. Holocene sediment types and their distribution in the southern Persian Gulf. In: PURSER, B.H. (ed), *The Persian Gulf, Holocene Carbonate Sedimentation and Diagenesis in a Shallow Epicontinental Sea*: 23-155.
- WALLISER, O., BULTYNCK, P., WEDDIGE, K., BECKER, R. & HOUSE, M., 1995. Definition of the Eifelian / Givetian Stage Boundary. *Episodes*, 18: 107-115.
- WILSON, J.L., 1975. *Carbonate Facies in Geologic History*. Springer Verlag, Berlin, 471 pp.
- ZBIKOWSKA, B., 1983. Middle to Upper Devonian Ostracods from northwestern Poland and their stratigraphic significance. *Palaeontologica Polonica*, 44, 108 pp.
- ZEGERS, T.E., DEKKERS, M.J. & BAILLY, S., 2003. Late Carboniferous to Permian remagnetization of Devonian limestones in the Ardennes: role of temperature, fluids, and deformation. *Journal of Geophysical Research*, 108 (B7): 2357.
- ZWING, A., MATZKA, J., BACHTADSE, V. & SOFFEL, H., 2005. Rock magnetic properties of remagnetized Palaeozoic clastic and carbonate rocks from the NE Rhenisch Massif, Germany. *Geophysical Journal International*, 160: 477-486.

Jean-Georges CASIER  
 Département de Paléontologie  
 Section Micropaléontologie-Paléobotanique  
 Institut royal des Sciences naturelles de Belgique  
 Rue Vautier, 29, B-1000 Bruxelles, Belgique  
 E-mail: casier@naturalsciences.be

Xavier DEVLEESCHOUWER  
 Service géologique de Belgique  
 Institut royal des Sciences naturelles de Belgique  
 Rue Jenner, 13, B-1000 Bruxelles, Belgique  
 E-mail: xavier.devleeschouwer@naturalsciences.be

Estelle PETITCLERC  
 Service géologique de Belgique  
 Institut royal des Sciences naturelles de Belgique  
 Rue Jenner, 13, B-1000 Bruxelles, Belgique  
 E-mail: estelle.petitclerc@naturalsciences.be

Alain PRÉAT  
 Département des Sciences de la Terre et de  
 l'Environnement  
 Université libre de Bruxelles CP 160  
 Av. F. D. Roosevelt, 50, B-1050 Bruxelles, Belgique  
 E-mail: acreat@ulb.ac.be

Typescript submitted: November 30, 2010.  
 Revised typescript received: June 17, 2011

#### ANNEXE 1

A list of Givetian ostracods figured by COEN (1985) and recently lodged with the collection of the Department of Paleontology of the Belgian royal Institute of natural Sciences. The numbering (IRScNB n° b 54...) is new. Ostracod specimens from the Mont d'Haurs are printed in bold.

- b5451. *Kozlowskiella rugulosa* (KUMMEROW, 1953). Pl. 1, Fig. 1;
- b5452. *Kozlowskiella rugulosa* (KUMMEROW, 1953). Pl. 1, Fig. 2;
- b5453. *Kozlowskiella rugulosa* (KUMMEROW, 1953). Pl. 1, Fig. 3;
- b5454. *Kozlowskiella* sp. Pl. 1, Fig. 4;
- b5455. *Falsipollex?* sp. Pl. 1, Fig. 5;
- b5456. *Tetrasacculus* sp.** Pl. 1, Fig. 6a,b;
- b5457. *Semibolbina* sp. Pl. 1, Fig. 7a,b;
- b5458. *Parapribylites hanaicus* POKORNY, 1950. Pl. 1, Fig. 8a-c;
- b5459. *Parapribylites hanaicus* POKORNY, 1950.** Pl. 1, Fig. 9;
- b5460. *Kielciella fastigans* (BECKER, 1964). Pl. 1, Fig. 10a,b;
- b5461. *Kielciella fastigans* (BECKER, 1964).** Pl. 1, Fig. 11;
- b5462. *Gravia schallreuteri* BECKER, 1970. Pl. 1, Fig. 12;
- b5463. *Gravia schallreuteri* BECKER, 1970. Pl. 1, Fig. 13;
- b5464. *Coryellina curta* (POLENOVA in ROZHDESTVENSKAJA, 1959).** Pl. 2, Fig. 1;
- b5465. *Coryellina curta* (POLENOVA in ROZHDESTVENSKAJA, 1959).** Pl. 2, Fig. 2;
- b5466. *Kielciella dorsi* ADAMCZAK, 1968? Pl. 2, Fig. 3a,b;
- b5467. *Kielciella dorsi* ADAMCZAK, 1968? Pl. 2, Fig. 4;
- b5468. *Urfella adamczaki* BECKER, 1970. Pl. 2, Fig. 5a,b;
- b5469. *Coryellina cybaea* ROZHDESTVENSKAJA, 1959. Pl. 2, Fig. 6;
- b5470. *Buregia ovata* (KUMMEROW, 1953). Pl. 2, Fig. 7;
- b5471. *Buregia ovata* (KUMMEROW, 1953).** Pl. 2, Fig. 8a,b;
- b5472. *Botzentia?* *solitaris solitaris* ADAMCZAK, 1968.** Pl. 2, Fig. 9;
- b5473. *Roundyella patagiata* (BECKER, 1964). Pl. 2, Fig. 10;
- b5474. *Roundyella patagiata* (BECKER, 1964).** Pl. 2, Fig. 11;
- b5475. *Refrathella cf. struvei* BECKER, 1967.** Pl. 2, Fig. 12;
- b5476. *Refrathella struvei* BECKER, 1967. Pl. 2, Fig. 13;
- b5477. *Refrathella struvei* BECKER, 1967.** Pl. 2, Fig. 14;
- b5478. *Refrathella cf. incompta* BECKER, 1971. Pl. 2, Fig. 15a,b;
- b5479. *Nodella faceta* ROZHDESTVENSKAJA, 1972. Pl. 3, Fig. 1;
- b5480. *Nodella faceta* ROZHDESTVENSKAJA, 1972. Pl. 3, Fig. 2;
- b5481. *Nodella hamata* BECKER, 1968. Pl. 3, Fig. 3;
- b5482. *Aechmina* sp.** Pl. 3, Fig. 4;
- b5483. *Coeloenellina minima* (KUMMEROW, 1953).** Pl. 3, Fig. 5a,b;
- b5484. *Coeloenellina cf. bijensis* (ROZHDESTVENSKAJA, 1959).** Pl. 3, Fig. 6;
- b5485. *Coeloenellina cf. bijensis* (ROZHDESTVENSKAJA, 1959).** Pl. 3, Fig. 7a,b, Fig. 4 in text;
- b5486. *Coeloenellina optata* (POLENOVA, 1955).** Fig. 5 in text;
- b5487. *Coeloenellina vellicata* n. sp.** Holotype. Pl. 3, Fig. 8a,b;
- b5488. *Coeloenellina vellicata* n. sp.** Paratype. Pl. 3, Fig. 9a,b;
- b5489. *Samarella aff. laevinodosa* BECKER, 1964.** Pl. 3, Fig. 10a,b;
- b5490. *Balantoides brauni* (BECKER, 1968). Pl. 3, Fig. 11;
- b5491. *Balantoides brauni* (BECKER, 1968). Pl. 3, Fig. 12;
- b5492. *Rectella trapezoides* ZASPELOVA, 1959? Pl. 3, Fig. 13a,b;
- b5493. *Evlanelia mitis* ADAMCZAK, 1968.** Pl. 3, Fig. 14;
- b5494. *Evlanelia mitis* ADAMCZAK, 1968.** Pl. 3, Fig. 15;
- b5495. *Evlanelia mitis* ADAMCZAK, 1968.** Pl. 3, Fig. 16;
- b5496. *Evlanelia mitis* ADAMCZAK, 1968.** Pl. 3, Fig. 17;
- b5497. *Poloniella tertia* KRÖMMELBEIN, 1953.** Pl. 4, Fig. 1;
- b5498. *Poloniella tertia* KRÖMMELBEIN, 1953.** Pl. 4, Fig. 2;
- b5499. *Poloniella tertia* KRÖMMELBEIN, 1953. Pl. 4, Fig. 3a,
- b; **b5500. *Poloniella claviformis* (KUMMEROW, 1953).** Pl. 4, Fig. 4a,b;
- b5501. *Uchtovia abundans* (POKORNY, 1950).** Pl. 4, Fig. 5a,b;
- b5502. *Uchtovia abundans* (POKORNY, 1950).** Pl. 4, Fig. 6a,b;
- b5503. *Uchtovia abundans* (POKORNY, 1950).** Pl. 4, Fig. 7;
- b5504. *Evlanelia germanica* BECKER, 1964.** Pl. 4, Fig. 8;
- b5505. *Evlanelia germanica* BECKER, 1964.** Pl. 4, Fig. 9;
- b5506. *Evlanelia germanica* BECKER, 1964.** Pl. 4, Fig. 10;
- b5507. *Evlanelia fibulaeformis* (ROZHDESTVENSKAJA, 1959). Pl. 4, Fig. 11;
- b5508. *Uchtovia refrathensis* (KRÖMMELBEIN, 1954). Pl. 5, Fig. 1a,b;

- b5509. *Uchtovia refrathensis* (KRÖMMELBEIN, 1954). Pl. 5, Fig. 2a,b;
- b5510. *Uchtovia refrathensis* (KRÖMMELBEIN, 1954). Pl. 5, Fig. 3;
- b5511. *Cavellina macella* KUMMEROW, 1953. Pl. 5, Fig. 4a,b;
- b5512. *Cavellina macella* KUMMEROW, 1953. Fig. 6 in textu;
- b5513. *Cavellina rhenana* KUMMEROW, 1953. Pl. 5, Fig. 5;
- b5514. *Cavellina rhenana* KUMMEROW, 1953. Pl. 5, Fig. 6;
- b5515. *Cavellina rhenana* KUMMEROW, 1953. Pl. 5, Fig. 7;
- b5516. *Cavellina rhenana* KUMMEROW, 1953. Pl. 5, Fig. 8;
- b5517. *Cavellina?* *wahlensis* n. sp. Holotype. Pl. 5, Fig. 9a,b;
- b5518. *Cavellina?* *wahlensis* n. sp. Paratype. Pl. 5, Fig. 10a,b;
- b5519. *Cavellina?* *wahlensis* n. sp. Fig. 7 in textu;
- b5520. *Cavellina devoniana* EGOROV, 1950. Pl. 5, Fig. 11a,b;
- b5521. *Cavellina devoniana* EGOROV, 1950. Pl. 5, Fig. 12a,b;
- b5522. "Healdianella" *budensis* OLEMPSKA, 1979. Fig. 8 in textu;
- b5523. *Polyzygia symmetrica* GÜRICH, 1896.** Pl. 6, Fig. 1;
- b5524. *Polyzygia beckmanni* KRÖMMELBEIN, 1954. Pl. 6, Fig. 2;
- b5525. *Quasillites fromelennensis* MILHAU, 1983. Pl. 6, Fig. 3a,b.
- b5526; *Quasillites fromelennensis* MILHAU, 1983. Pl. 6, Fig. 4;
- b5527. *Quasillites lecomptei* n. sp. Paratype.** Pl. 6, Fig. 5;
- b5528. *Quasillites lecomptei* n. sp. Holotype.** Pl. 6, Fig. 6;
- b5529. *Jenningsina paffrathensis* KRÖMMELBEIN, 1954. Pl. 6, Fig. 7;
- b5530. *Jenningsina heddebauti* MILHAU, 1983.** Pl. 6, Fig. 8;
- b5531. *Jefina kaisini* n. sp. Holotype. Pl. 6, Fig. 9a-c;
- b5532. *Jefina kaisini* n. sp. Paratype. Pl. 6, Fig. 10;
- b5533. *Jefina kaisini* n. sp. Paratype. Pl. 6, Fig. 11;
- b5534. Indéterminé. Pl. 6, Fig. 12;
- b5535. *Parathurammina*. Pl. 6, Fig. 13;
- b5536. *Jefina romei* n. sp.** Holotype. Pl. 6, Fig. 14a,b;
- b5537. *Jefina romei* n. sp. Paratype. Pl. 6, Fig. 15;
- b5538. *Jefina romei* n. sp. Paratype. Pl. 6, Fig. 16;
- b5539. *Jefina romei* n. sp. Paratype. Pl. 6, Fig. 17;
- b5540. *Zeuschnerina dispar* ADAMCZAK, 1976. Pl. 6, Fig. 18;
- b5541. *Leptoprimitia* sp.** Pl. 6, Fig. 19;
- b5542. *Buflina* aff. *abbreviata* PETERSON, 1966. Pl. 7, Fig. 1;
- b5543. *Buflina* aff. *abbreviata* PETERSON, 1966. Pl. 7, Fig. 2;
- b5544. *Buflina schaderthalensis* ZAGORA, 1968. Pl. 7, Fig. 3;
- b5545. *Buflina schaderthalensis* ZAGORA, 1968.** Pl. 7, Fig. 4a,b;
- b5546. *Buflina schaderthalensis* ZAGORA, 1968. Pl. 7, Fig. 5;
- b5547. *Buflina schaderthalensis* ZAGORA, 1968.** Pl. 7, Fig. 6;
- b5548. *Buflina schaderthalensis* ZAGORA, 1968. Pl. 7, Fig. 7;
- b5549. *Ropolonellus* cf. *aznajevaensis* (ROZHDESTVENSKAJA, 1962). Pl. 7, Fig. 8;
- b5550. *Ropolonellus* cf. *aznajevaensis* (ROZHDESTVENSKAJA, 1962). Pl. 7, Fig. 9;
- b5551. *Euglyphella europaea* n. sp. Paratype. Pl. 7, Fig. 10;
- b5552. *Euglyphella europaea* n. sp. Holotype. Pl. 7, Fig. 11a,b;
- b5553. *Euglyphella europaea* n. sp. Paratype. Pl. 7, Fig. 12;
- b5554. *Euglyphella europaea* n. sp. Paratype. Pl. 7, Fig. 13;
- b5555. *Euglyphella europaea* n. sp. Paratype. Pl. 7, Fig. 14;
- b5556. *Euglyphella europaea* n. sp. Paratype. Pl. 7, Fig. 15;
- b5557. *Euglyphella europaea* n. sp. Paratype. Pl. 7, Fig. 16;
- b5558. *Cytherellina obliqua* (KUMMEROW, 1953). Pl. 8, Fig. 1;
- b5559. *Cytherellina obliqua* (KUMMEROW, 1953). Pl. 8, Fig. 2;
- b5560. *Cytherellina obliqua* (KUMMEROW, 1953). Pl. 8, Fig. 3;
- b5561. *Cytherellina obliqua* (KUMMEROW, 1953). Pl. 8, Fig. 4;
- b5562. *Cytherellina obliqua* (KUMMEROW, 1953). Pl. 8, Fig. 5;
- b5563. *Cytherellina obliqua* (KUMMEROW, 1953).** Pl. 8, Fig. 6;
- b5564. *Cytherellina obliqua* (KUMMEROW, 1953).** Pl. 8, Fig. 7;
- b5565. *Cytherellina obliqua* (KUMMEROW, 1953).** Pl. 8, Fig. 8;
- b5566. *Cytherellina groosae* n. sp. Paratype. Pl. 8, Fig. 9;
- b5567. *Cytherellina groosae* n. sp. Holotype. Pl. 8, Fig. 10;
- b5568. *Cytherellina groosae* n. sp. Paratype. Pl. 8, Fig. 11;
- b5569. *Cytherellina groosae* n. sp. Paratype. Pl. 8, Fig. 12;
- b5570. *Cytherellina* sp. Pl. 8, Fig. 13;
- b5571. *Cytherellina* sp. Pl. 8, Fig. 14;
- b5572. *Cytherellina* sp. Pl. 8, Fig. 15;
- b5573. *Cytherellina* sp. Pl. 8, Fig. 16;
- b5574. *Cytherellina?* *dubia* (KUMMEROW, 1953). Pl. 8, Fig. 17;
- b5575. *Bairdia paffrathensis* KUMMEROW, 1953. Pl. 8, Fig. 18;
- b5576. *Bairdia paffrathensis* KUMMEROW, 1953. Pl. 8, Fig. 19a,b;
- b5577. *Bairdia* cf. *paffrathensis* KUMMEROW, 1953.** Pl. 8, Fig. 20;
- b5578. *Bairdia* cf. *paffrathensis* KUMMEROW, 1953. Pl. 8, Fig. 21;
- b5579. *Cryptophyllus* sp 1. Pl. 8, Fig. 22;
- b5580. *Cryptophyllus* sp 2. Pl. 8, Fig. 23;
- b5581. *Bairdia* cf. *siliklensis* ROZHDESTVENSKAJA, 1962.** Pl. 9, Fig. 1;
- b5582. *Bairdia* cf. *siliklensis* ROZHDESTVENSKAJA, 1962.** Pl. 9, Fig. 2;
- b5583. *Bairdia* cf. *siliklensis* ROZHDESTVENSKAJA, 1962.** Pl. 9, Fig. 3;
- b5584. *Bairdia* cf. *siliklensis* ROZHDESTVENSKAJA, 1962.** Pl. 9, Fig. 4;
- b5585. *Baidiocyparis corniger* ROZHDESTVENSKAJA, 1962. Pl. 9, Fig. 5;
- b5586. *Bairdia* cf. *carinata* POLENOVA, 1960. Pl. 9, Fig. 6;
- b5587. *Bairdia* cf. *carinata* POLENOVA, 1960.** Pl. 9, Fig. 7a,b;
- b5588. *Microcheilinella* aff. *ventrosa* POLENOVA, 1960.** Pl. 9, Fig. 8a,b;
- b5589. *Microcheilinella* affinis POLENOVA, 1955.** Pl. 9, Fig. 9;

- b5590. *Microcheilinella affinis* POLENOVA, 1955. Pl. 9, Fig. 10;  
**b5591.** *Bairdiocypris symmetrica* (KUMMEROW, 1953). Pl. 9, Fig. 11;  
b5592. *Bairdia* sp. Pl. 9, Fig. 12;  
b5593. *Bairdiacypris* sp. Pl. 9, Fig. 13;  
b5594. *Microcheilinella* sp. Pl. 9, Fig. 14;
- b5595. *Microcheilinella* sp. Pl. 9, Fig. 15;  
**b5596.** *Orthocypris cicatricosa* n. sp. Paratype. Pl. 9, Fig. 16;  
b5597. *Orthocypris cicatricosa* n. sp. Holotype. Pl. 9, Fig. 17a,b;  
b5598. *Orthocypris cicatricosa* n. sp. Paratype. Pl. 9, Fig. 18;  
b5599. *Orthocypris cicatricosa* n. sp. Paratype. Pl. 9, Fig. 19;  
**b5600.** *Saumella* sp. Pl. 9, Fig. 20.

### Explanation of plates

All types are deposited in the collections of the Department of Paleontology (section Micropaleontology) of the Royal Belgian Institute of natural Sciences (IRScNB n° b 54...). Thin sections are deposited in the Department of Earth Sciences and Environment of the University of Brussels (ulb/sed ...). MH = sample number (see Fig. 2 for the stratigraphic position). Ha Fm = Hanonet Fm; TF Fm = Trois-Fontaines Fm.

#### PLATE 1

- Fig. 1 — *Amphissites tener omphalotus* BECKER, 1964, MH-503, Ha Fm, IRScNB n° b 5397, left valve, x60.  
Fig. 2 — *Parabolbinella coeni* n. sp., MH-501, Ha Fm, IRScNB n° b 5398, left valve of heteromorph, x45.  
Fig. 3 — *Kozlowskiella* sp. C in CASIER et al. (1994), MH-543, TF Fm, IRScNB n° b 5399, right valve, x45.  
Fig. 4 — *Fellerites crumena* (KUMMEROW, 1953), MH-527, Ha Fm, IRScNB n° b 5400, right valve, x35.  
Fig. 5 — *Kielciella* cf. *fastigans* (BECKER, 1964), MH-543, TF Fm, IRScNB n° b 5401, right valve, x55  
Fig. 6 — *Parapribylites hanaicus* POKORNY, 1950, MH-612, TF Fm, IRScNB n° b 5402, right lateral view of the carapace of a tecnomorph, x85.  
Fig. 7 — *Aparchites* sp. A in CASIER et al. (2010), MH-525, Ha Fm, IRScNB n° b 5403, right lateral view of a carapace, x50.  
Figs 8-10 — *Coryellina?* *audiarti* nov. sp. 8. Holotype, a. Right lateral view, x70, b. Dorsal view, x55, 9. Right lateral view of Paratype A, x75, 10. Right lateral view of Paratype B, x65.  
Fig. 11 — *Urfstella adamczacki* BECKER, 1970, MH-501, Ha Fm, IRScNB n° b 5407, right lateral view of a carapace, x45.  
Fig. 12 — *Refrathella struvei* BECKER, 1967, MH-501, Ha Fm, IRScNB n° b 5408, left valve, x80.  
Fig. 13 — *Roundyella patagiata* (BECKER, 1964), MH-503, Ha Fm, IRScNB n° b 5409, broken valve, x60.  
Fig. 14 — *Samarella* cf. *laevinodosa* BECKER, 1964, MH-523, Ha Fm, IRScNB n° b 5410, right lateral view of a carapace, x65.  
Fig. 15 — *Buregia ovata* (KUMMEROW, 1953), MH-525, Ha Fm, IRScNB n° b 5411, right lateral view of carapace, x70.  
Fig. 16 — *Coeloenellina minima* (KUMMEROW, 1953), MH-612, TF Fm, IRScNB n° b 5412, left lateral view of a carapace, x50.  
Fig. 17 — *Coeloenellina* sp. A, aff. *minima* (KUMMEROW, 1953), MH-612, TF Fm, IRScNB n° b 5413, right lateral view of a carapace, x40.  
Fig. 18 — *Coeloenellina?* sp. indet., MH-527, Ha Fm, IRScNB n° b 5414, right lateral view of a carapace, x65.

#### PLATE 2

- Fig. 1 — *Poloniella tertia* KRÖMMELBEIN, 1953, MH-502, Ha Fm, IRScNB n° b 5415, right lateral view of a carapace, x60.  
Fig. 2 — *Poloniella* cf. *claviformis* (KUMMEROW, 1953), MH-502, Ha Fm, IRScNB n° b 5416, poorly preserved right valve, x75.  
Fig. 3 — *Marginia* cf. *sculpta multicostata* POLENOVA, 1953, MH-503, Ha Fm, IRScNB n° b 5417, left valve, x80.  
Fig. 4 — *Cavellina macella* (KUMMEROW, 1953)?, MH-604, TF Fm, IRScNB n° b 5418, right lateral view of a poorly preserved carapace, x80.  
Figs 5-6 — *Cavellina haursensis* nov. sp., 5. Holotype, a. Right lateral view, x50, b. Dorsal view, x45, 6. Right lateral view of Paratype A, x65.  
Fig. 7 — *Uchtovia kloedenellides* (ADAMCZAK, 1968), MH-503, Ha Fm, IRScNB n° b 5422, left lateral view of a broken carapace, x60.

- Fig. 8-9 — *Uchtovia abundans* (POKORNY, 1950), 8. MH-502, Ha Fm, IRSNB n° b 5423, left lateral view of the carapace of a juvenile, x70, 9. MH-503, Ha Fm, IRSNB n° b 5424, left lateral view of a carapace, x45.
- Figs 10-11 — *Svantovites primus* POKORNY, 1950, 10. MH-507, Ha Fm, IRSNB n° b 5425, right lateral view of a carapace, x75, 10. MH-507, Ha Fm, IRSNB n° b 5426, a. Right lateral view of a carapace with removed right valve, x75, b. Removed right valve, x80.
- Fig. 12 — *Jefina romei* COEN, 1985?, MH-501, Ha Fm, IRSNB n° b 5427, right lateral view of a carapace, x70.
- Fig. 13 — *Bufina schaderthalensis* ZAGORA, 1968, MH-500, Ha Fm, IRSNB n° b 5428, right lateral view of carapace, x55.
- Fig. 14 — *Ropolonellus ketneri* (POKORNY, 1950), MH-503, Ha Fm, IRSNB n° b 5429, right lateral view of a carapace, x70.
- Fig. 15 — *Cytherellina obliqua* (KUMMEROW, 1953), MH-501, Ha Fm, IRSNB n° b 5430, right lateral view of a carapace, x65.
- Fig. 16 — *Cytherellina?* cf. *brassicalis* BECKER, 1965, MH-501, Ha Fm, IRSNB n° b 5431, right lateral view of a carapace, x45.
- Fig. 17 — *Cytherellina perlonga* (KUMMEROW, 1953), MH-523, Ha Fm, IRSNB n° b 5432, right lateral view of a carapace, x70.

## PLATE 3

- Fig. 1 — *Cytherellina* sp. A, MH-508, Ha Fm, IRSNB n° b 5433, right lateral view of a carapace, x85.
- Fig. 2 — *Cytherellina?* sp. indet., MH-507, Ha Fm, IRSNB n° b 5434, right lateral view of a carapace, x75.
- Fig. 3 — *Healdianella* sp. A, aff. *budensis* OLEMPSKA, 1979, MH-527, Ha Fm, IRSNB n° b 5435, right lateral view of a carapace, x85.
- Fig. 4 — *Bairdiocypris rauffi* KRÖMMELBEIN, 1952, MH-503, Ha Fm, IRSNB n° b 5436, right lateral view of a carapace, x20.
- Fig. 5 — *Bairdiocypris* cf. *symmetrica* (KUMMEROW, 1953), MH-501, Ha Fm, IRSNB n° b 5437, poorly preserved right valve, x55.
- Fig. 6 — *Bairdiocypris* sp. A, aff. *eifliensis* (KEGEL, 1928), MH-507, Ha Fm, IRSNB n° b 5438, right lateral view of a carapace, x60.
- Fig. 7 — *Baschkirina* sp. B in CASIER et al. (1992)?, MH-523, Ha Fm, IRSNB n° b 5439, right lateral view of a poorly preserved carapace, x35.
- Fig. 8 — “*Orthocypris*” sp. in CASIER et al. (1995), MH-505, Ha Fm, IRSNB n° b 5440, right lateral view of a carapace, x65.
- Fig. 9 — *Microcheilinella affinis* POLENOVA, 1955, MH-525, Ha Fm, IRSNB n° b 5441, right lateral view of a carapace, x85.
- Fig. 10 — *Tubulibairdia clava* (KEGEL, 1933), MH-523, Ha Fm, IRSNB n° b 5442, right lateral view of a carapace, x35.
- Fig. 11 — *Acratia* sp. A, aff. *Cechelovites cultratus* POKORNY, 1950, MH-502, Ha Fm, IRSNB n° b 5443, right lateral view of a poorly preserved carapace, x50.
- Fig. 12 — *Bairdia paffrathensis* KUMMEROW, 1953, MH-502, Ha Fm, IRSNB n° b 5444, right lateral view of a carapace, x45.
- Fig. 13 — *Bairdia* cf. *carinata* POLENOVA, 1960, sensu COEN (1985), MH-525, Ha Fm, IRSNB n° b 5445, right lateral view of a poorly preserved carapace, x40.
- Fig. 14 — *Bairdia* cf. *tischendorfi* BECKER, 1965, MH-507, Ha Fm, IRSNB n° b 5446, right lateral view of poorly preserved carapace, x40.
- Fig. 15 — *Bairdia* sp. A, MH-503, Ha Fm, IRSNB n° b 5447, right lateral view of a carapace, x45.
- Fig. 16 — *Bairdia* sp. B, MH-525, Ha Fm, IRSNB n° b 5448, right lateral view of a poorly preserved carapace, x70.
- Fig. 17 — *Bairdiacypris antiqua* (POKORNY, 1950), MH-608, TF Fm, IRSNB n° b 5449, right lateral view of poorly preserved carapace, x45.
- Fig. 18 — *Cryptophyllus* sp. indet., MH-608, TF Fm, IRSNB n° b 5450, poorly preserved valve, x50.

## PLATE 4

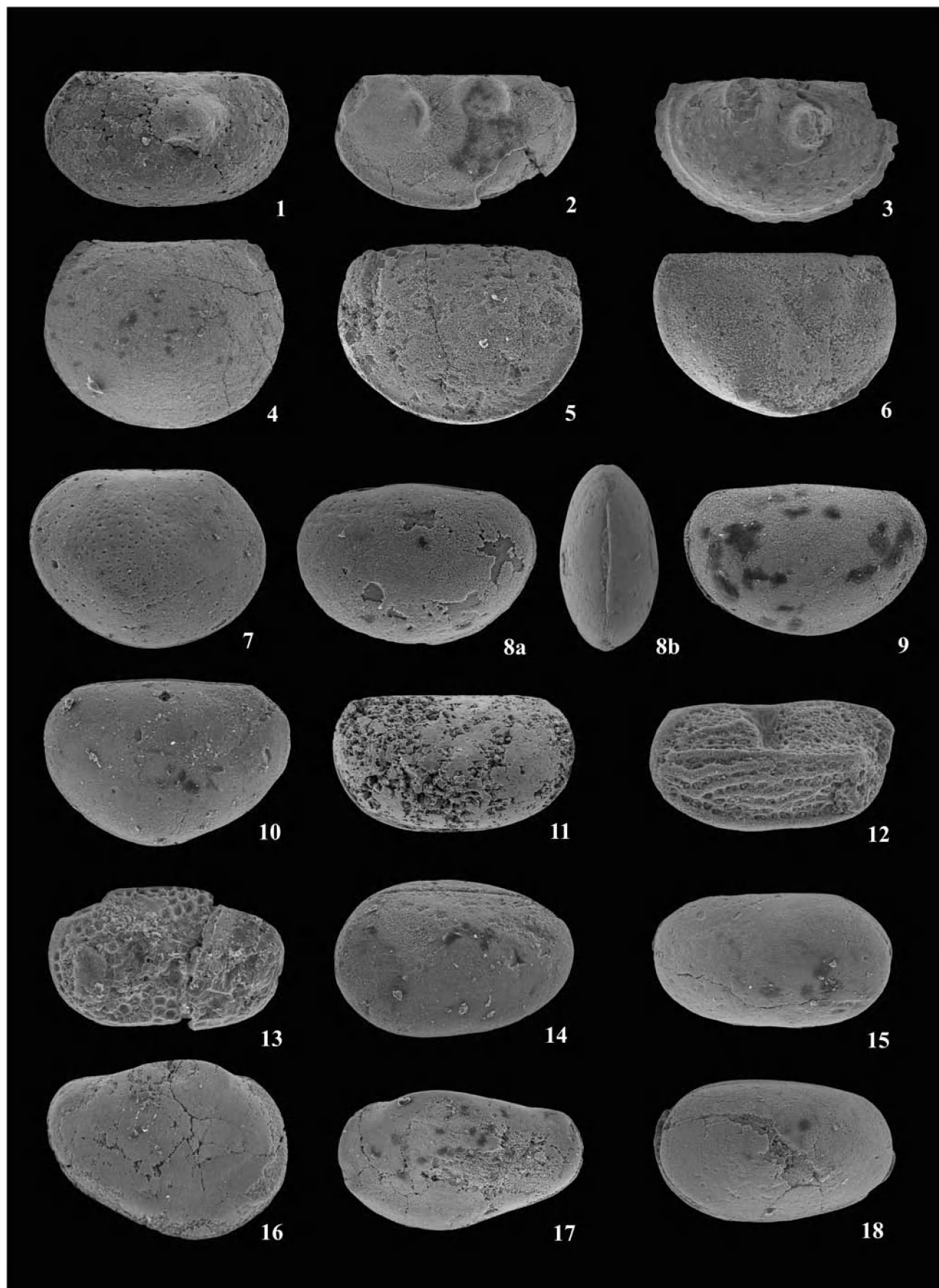
## Open marine environment

- Figs 1-2 — Burrowed bioclastic (echinoderms, bryozoa, cricoconarids, ostracods) wackestone with a slightly recrystallized fine-grained calcitic microspar. Blackish zones are filamentous, spheroidal pyrite (Fig. 2) accumulated along the pressure solution seams (Fig. 1). Open-marine environment near the storm-wave base-level. MF2, ulb/sed 6836-10 (Fig. 1) and 6837-10 (Fig. 2), MH-501, Ha Fm.
- Figs 3-5 — *Girvanella* oncoid developed on a coral fragment (tabulata) in a bioclastic packstone (Fig. 3). See multiple envelope (here two layers are visible, a blackish one encrusted by a greyish one). *Girvanella* can bind the bioclasts (crinoids in the Fig. 4 or brachiopods and bryozoa in the Fig. 5). Framboidal pyrite is trapped in the *Girvanella* mats (Fig. 5). Open marine environment with intermittent agitation near the storm-wave base level. MF3, ulb/sed 6825-10 (Fig. 3), 6830-10 (Fig. 4) and 6827-10 (Fig. 5), MH-508, Ha Fm.
- Fig. 6 — Bioclastic packstone with a brachiopod shell and slightly altered crinoids. Undeterminable microbioclasts are present between the bioclasts and crinoids, and mixed in the microparitized calcite matrix. The punctae of the brachiopod are filled with very small-sized pyrite spheres. The peloid below the brachiopod shell is a micritized *Girvanella* fragment. Irregular pressure solution seams are observed between the bioclasts. Open marine environment near the storm-wave base level. MF3, ulb/sed 6845-10, MH-507, Ha Fm.
- Figs 7-8 — Stromatoporoid floatstone with a bioclastic (issinellids, Fig. G; crinoids, Fig. H) packstone matrix. Peloids and crinoids exhibit an oblique stratification and a few crinoidal fragment with a syntaxial cement (centre of the photo). Agitated peri-reefal environment near a bioconstruction. MF4, ulb/sed 6884-10 (Fig. 7) and 6893-10 (Fig. 8). MH-600, TF Fm.

## PLATE 5

## Fore-shoal and restricted lagoonal environments

- Fig. 1 — Peloidal molluscan-crinalid packstone. Former geopetal infillings in the gastropods. The large bioclasts represent a storm layer in a peloidal wackestone-packstone. Open marine fore-shoal near the fair-weather wave-base level. MF5, ulb/sed 6848-10, MH-513, Ha Fm.
- Fig. 2 — Peloidal bioclastic packstone with *Bisphaera* Birina, 1948 (*incertae sedis*). The matrix is a medium-grained calcite microsparite. Open marine fore-shoal near the fair-weather wave-base level. MF5, ulb/sed 6856-520, MH-513, TF Fm.
- Fig. 3 — Calcispherid (*Calcisphaera*) wackestone ("calcispherite") with *Kamaena* (alga) and an ostracod valve in a dense dark micrite. Restricted lagoon. MF8, ulb/sed 6909-10, MH-609, TF Fm.
- Fig. 4 — Peloidal calcispherid (*Parathurammina dagmarae*) wackestone ("calcispherite"). The matrix is slightly recrystallized and most of the white calcite comes from the dissolution of molluscs. Restricted lagoon. MF8, ulb/sed 6915-10, MH-610, TF Fm.
- Fig. 5 — Homogeneous wackestone with Leperditicopid valves overlain by an issinellid (alga). Framboidal pyrite in the dense micritic matrix. Restricted lagoon. MF9, ulb/sed 6918-10, MH-611, TF Fm.
- Fig. 6 — Abundant bipyramidal quartz microcrystals with tiny micritic inclusions. The dense micritic matrix contains a few peloids and one strongly altered (microsparitized) pelecypod fragment (upper left corner of the photo). MF9, ulb/sed 6869-10, MH-539, TF Fm.
- Figs 7-8 — Wackestone with an umbrella "cavity" giving upward a particular fenestrae starting from the base of a gastropod (Fig. 7). The fenestra is filled with yellowish thick fibrous and white granular calcitic cements. The dense micritic matrix contains abundant microparitized (fine-grained calcite microspar) sponge spicules (Fig. 8). The photo displays an ostracod valve. Restricted lagoon. MF11, ulb/sed 6877-10 (Fig. 7) and 6871-10 (Fig. 8) MH-540, TF Fm.



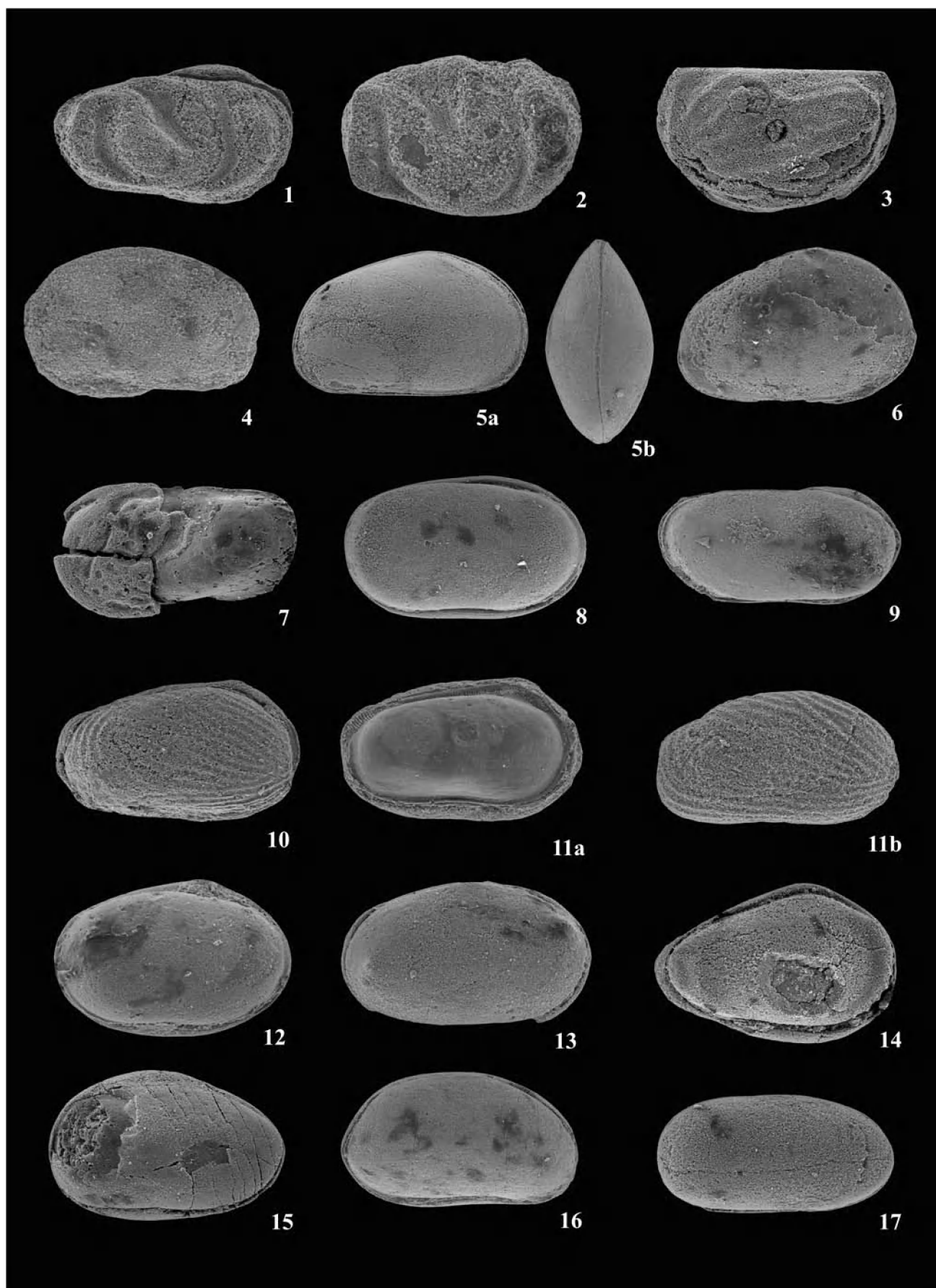


PLATE 2

